Open Access

Recent Progress in Materials

LIDSEN Publishing Inc.

Review

Review on the Development of Titanium Diboride Ceramics

Xinran Lv [1, 2], Ziqiang Yin [1, 2], Zhigang Yang [1, 2, *], Junshuai Chen [1, 2], Shen Zhang [1, 2], Shaolei Song [3], Gang Yu [1, 2]

1. School of Materials Science and Engineering, Hebei Provincial Key Laboratory of Traffic Engineering Materials, Shijiazhuang Tiedao University, Shijiazhuang 050043, China; E-Mails: 1202108047@student.stdu.edu.cn; yinziqiang@nimte.ac.cn; yangzhigang@stdu.edu.cn; 1202208029@student.stdu.edu.cn; 1202208075@student.stdu.edu.cn; yugang@stdu.edu.cn
2. Hebei Provincial Engineering Research Center of Metamaterial and Micro-device, Shijiazhuang Tiedao University, Shijiazhuang, 050043, China
3. School of Civil Engineering, Xuzhou University of Technology, Xuzhou 221018, China; E-Mail: songshaolei@xzit.edu.cn

***Correspondence:** Zhigang Yang; E-Mail: yangzhigang@stdu.edu.cn

Academic Editor: Ali Abdul-Aziz

Special Issue: Ceramic Matrix Composites: Performance Evaluation and Application

Recent Progress in Materials
2024, volume 6, issue 2
doi:10.21926/rpm.2402009

Received: January 02, 2024
Accepted: March 27, 2024
Published: April 03, 2024

Abstract

Titanium diboride (TiB_2) materials have garnered significant attention due to their remarkable comprehensive properties. They offer potential applications in high-temperature structural materials, cutting tools, armor, electrodes for metal smelting, and wear-resistant parts. However, due to the low self-diffusion coefficient, the TiB_2 exhibits poor sinterability, excessive grain growth at elevated temperatures, and inadequate oxidation resistance, limiting its wide application. Therefore, many research works are devoted to processing TiB_2 at a lower sintering temperature and improving the properties through various sintering additives and more advanced techniques. This article comprehensively reviews the multiple synthesis methods and sintering technologies of TiB_2, and at the same time, critically discusses

the impacts of sintering additives and reinforcing agents on densification, microstructure, and various properties, including those at high temperatures, and finally predicts the future development of TiB_2 composite materials.

Keywords
TiB_2; synthesis methods; sintering technologies; densification; properties

1. Introduction

It is well known that ceramic materials can exhibit some superior properties concerning metals, such as excellent thermal stability, corrosion resistance, and wear resistance [1]. Because of these properties, they are regarded as promising for high-temperature structural applications. Among these high-temperature ceramics, ceramics with melting points>3000°C are generally considered to be Ultra High-Temperature Ceramics (UHTCs) [2, 3]. UHTCs encompass borides, carbides, and nitride compounds derived from the periodic table's transition metals of groups IVB and VB. Compared with other ceramic materials, due to their high melting points, superior mechanical properties, and excellent chemical stability, UHTCs have garnered attention for potential use in high-temperature structural applications, such as aerospace, where high-temperature resistance is required [4-9].

Among these UHTCs, transition metal borides, especially titanium diboride (TiB_2), have been extensively researched, and their basic properties have been shown in Table 1. TiB_2 exhibits both metal-like and ceramic-like properties. TiB_2 ceramics are characterized by an excellent combination of properties, including a high melting point (>3000°C), high hardness (about 25-35 GPa at room temperature, very close to diamond, cubic boron nitride and boron carbide), low density (4.52 g/cm^3), excellent electrical conductivity, good thermal conductivity (60-120 $W\cdot(m\cdot K)^{-1}$), superior chemical stability (excellent stability in contact with Al or Fe at high temperature) and other exceptional physical and chemical properties [4, 8, 10]. Table 1 compares the critical physical and mechanical properties of high-temperature ceramics. It can be noted that among these materials, TiB_2 exhibits more excellent mechanical properties. This unique combination of titanium diboride is beneficial to the performance of a wide range of technology applications, such as in cutting tools, wear-resisting components, metal melting crucibles, light armor, cathode material for salt-bath electrolysis in aluminum production and other fields [10]. In addition, TiB_2 can not only be used as matrix material but also can be used as a strengthening ceramic phase to enhance other mechanical properties such as the strength and toughness of different materials, such as SiC-TiB_2 [11], B_4C-TiB_2-SiC [12], etc. Therefore, to clearly understand the research progress of TiB_2 ceramics and related composites, a comprehensive conclusion should be given. This review primarily focuses on crystal structure, synthesis methods, sintering techniques, densification, microstructure, and mechanical properties of TiB_2 ceramics. Finally, a brief overview of existing and futuristic applications and some future challenges are presented.

Table 1 Properties of TiB_2 and other important high-temperature ceramics.

Properties	TiB_2 [4, 9]	ZrB_2 [13, 14]	TiC [15, 16]	TiN [17, 18]	Al_2O_3 [4]	WC [4]
Crystal structure	HCP	HCP	FCC	FCC	HCP	HCP
Melting point (°C)	3225	3200	3100	2950	2043	2600
Density (g/cm^3)	4.5	6.1	4.9	5.4	3.99	15.7
CTE (α; 10^{-6} K^{-1})	8.6	6.8	7.7	9.3	8.0	5.2-7.3
Thermal conductivity (W m^{-1} K^{-1})	60-120	60	17-32	19.2	30.1	29-121
Electrical resistivity (10^{-6} Ω·cm)	9-15	10-32	68	22	10^{20}	17
Elastic modulus (GPa)	500-560	340-500	451	-	400	720
Hardness (GPa)	25-35	20-25	24-32	8-9	18-21	20-24
Fracture toughness (MPa·m$^{1/2}$)	4-5	4	4	-	2.5-4	
Flexural strength (MPa)	700-1000	300-400	240-270	-	323	480-830
Oxidation resistance (°C)	<1200	1200-1400	1200	-	>1700	800

2. Phase Diagram and Crystal Structure of TiB_2

Three intermetallic phases exist in the Ti-B binary system: orthorhombic Ti_3B_4, orthorhombic TiB, and hexagonal TiB_2 (as depicted in Figure 1). These phases decompose at distinct peritectic temperatures. Specifically, Ti_3B_4 and TiB undergo phase decomposition at 2180°C and 2200°C, respectively, while TiB_2 undergoes congruent melting at 3225°C. TiB and TiB_2 phases have a narrow homogeneity range, while Ti_3B_4 maintains a fixed composition. TiB_2 shows formation stability in a stoichiometric range of 28.5 to 30 percent by weight of B. Owing to the highest melting point of TiB_2, it is considered to be an essential candidate material for high-temperature structural applications [19, 20].

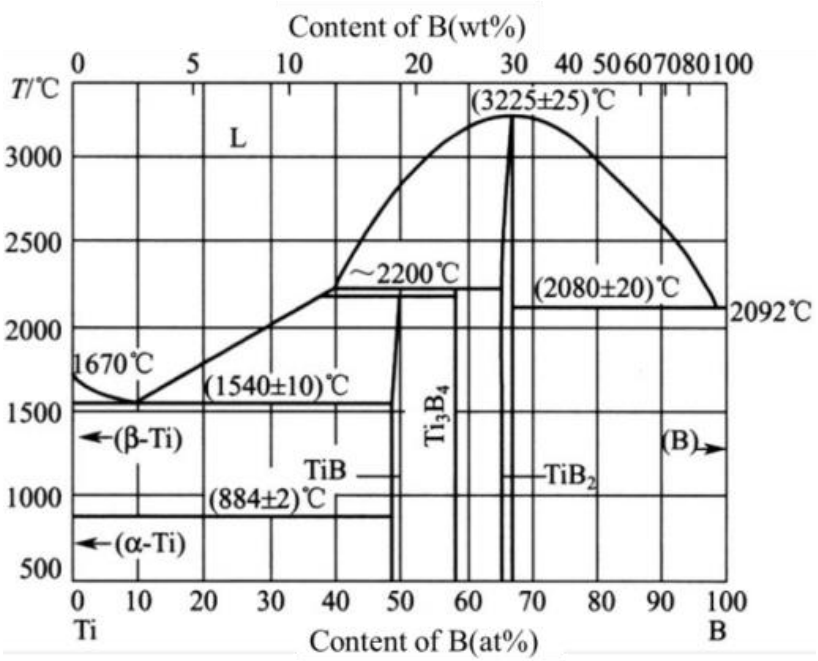

Figure 1 Ti-B binary equilibrium phase diagram indicates the possibility of forming three intermetallic compounds: TiB, Ti_3B_4 and TiB_2 [20].

The composition of borides is notably influenced by critical factors, primarily the atomic ratio between boron (B) and metal (M). Generally, the B:M ratios range from 1:4 to 12:1. This ratio significantly impacts both the electronic structure and inherent properties of these compounds. Elevating the quantity of B atoms within the structure enhances the strength of B-B bonds, consequently elevating melting temperatures, hardness, strength, and chemical stability. Moreover, the strength of M-B bonds in diborides is contingent upon the degree of electron localization surrounding the M atoms [19]. Concerning the crystal structure, TiB_2 has the primitive hexagonal crystal structure of the AlB_2 type, with space group of P6/mmm (a = b = 3.029 Å, c = 3.229 Å; α = β = 90°, γ = 120°), and there are three atoms in the unit cell, and all of them are on the unique positions: Ti atoms are located at (0,0,0) and B atoms at (1/3,2/3,1/2) and (2/3,1/3,1/2) lattice sites (Figure 2) [21-23]. In analogy with the usual hexagonal close-packed (HCP) structure, the metal layers are close-packed and stacked in an A-A-A sequence. The structural configuration comprises layers characterized by B atoms arranged in 2D graphite-like rings or networks, alternating with hexagonally close-packed Ti layers. Each Ti atom is encircled by six equidistant Ti neighbors within its plane, alongside 12 equidistant B neighbors—six positioned above and six below the Ti layer. Similarly, each B atom is surrounded by three neighboring B atoms within its plane, complemented by six Ti atoms—three positioned above and three below the B layer [24-26].

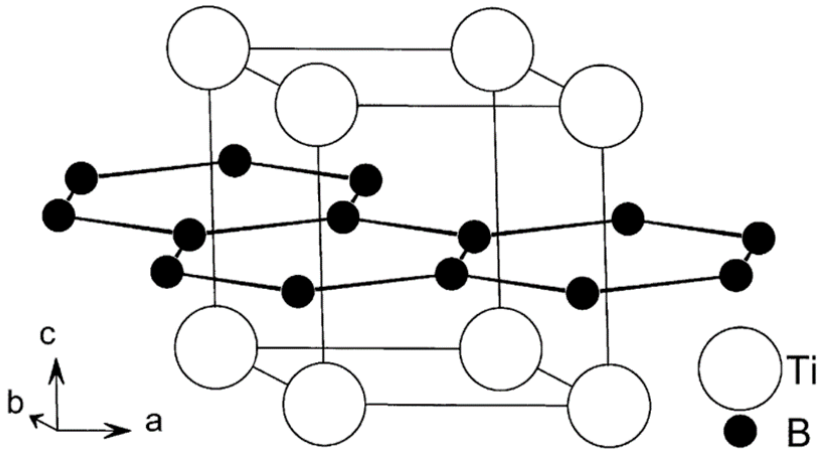

Figure 2 The hexagonal unit cell of single crystal TiB_2, (AlB_2-type, p6/mmm space group, a = b = 3.029 Å, c = 3.229 Å; α = β = 90°, γ = 120°), 1 formula unit per cell, Ti at (0,0,0), B at (1/3,2/3,1/2) and (2/3,1/3,1/2) and the hexagonal net of boron atoms [27].

Overall, the high hardness, elastic modulus, and excellent chemical resistance of TiB_2 are attributed to its intrinsic atomic bonding (Ti-Ti, B-B, and Ti-B) and crystal structure. However, the covalent bonding characteristic makes it very difficult to realize the densification, mainly owing to the low self-diffusion coefficient of TiB_2 caused by the immobility of Ti^+ and B^- ions during sintering [28].

3. Synthesis of Titanium Diboride Powders

The synthesis of powders dramatically influences the sintering properties of TiB_2, so the synthesis methods of powders are essential. Regarding sintering processes, the focus should be on acquiring finer TiB_2 powders characterized by a narrow particle size distribution and minimal agglomeration.

The presence of agglomerates in the sintered powders reduces sinterability and leads to micro/macro pores forming in sintered ceramics. Therefore, agglomeration is an essential problem in the synthesis of ceramic powders. In addition to the initial size of TiB_2 powders, the purity and oxygen content also significantly affect the sintering properties because they quickly cause the coarsening of TiB_2 grains [4]. Therefore, it is essential to have a good synthesis process of TiB_2 powders for subsequent sintering. At present, varieties of synthesis methods for TiB_2 powders are reported. According to the initial form of the reactants, these methods are divided into the gas phase, solid phase, and liquid phase method, and their classification and synthesis mechanisms are shown in Figure 3. For the gas phase method, the reaction between B supplied by B_2H_6 or BCl_3 and Ti supplied by $TiCl_4$ under the function of H_2 reduction will happen to form the TiB_2 powders. For the solid phase method, TiB_2 can be synthesized by the borothermic or borocarbothermic reduction reaction, among which TiO_2 was used as the Ti source, and B_2O_3, B, or B_4C was used as the B source, and C or B_4C were used as the C source (reducing agent). For the liquid phase method, such as precursor and sol-gel technologies, gel mixture can be formed by the reaction among B source, Ti source, and organic carbon source in a solvent, and they are further calcined to form TiB_2 powders.

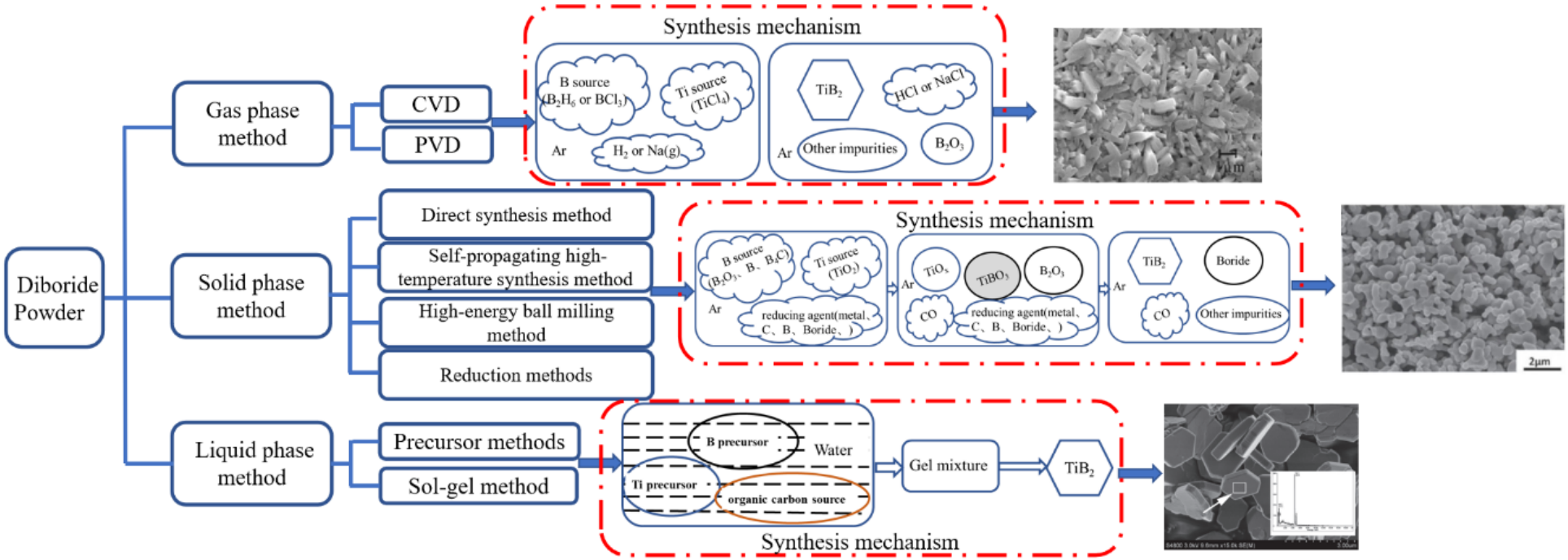

Figure 3 Diagram of powder synthesis methods and mechanism.

3.1 Gas Phase Method

The gas phase method was studied earlier in preparing TiB_2 films, mainly including the CVD, PVD, and other technologies developed on the corresponding basis (Figure 4a). Takehiko et al. [29] prepared TiB_2 films up to 100 μm by CVD in an ultrasonic field. It was found that the grain size of TiB_2 was significantly reduced after ultrasonic irradiation. It has been widely reported that a reaction of $NaBH_4$ and $TiCl_4$ can prepare the nanocrystalline TiB_2, and the powders can be obtained after high-temperature annealing [30-32]. Whereafter, Axelbaum developed a method in which nanometer-sized TiB_2 was synthesized by gas-phase combustion reactions of sodium vapor with $TiCl_4$ and BCl_3, and the grain size of TiB_2 was less than 15 nm in diameter [33]. Sure researchers synthesized TiB_2 (14-40 nm) utilizing a benzene-thermal reaction involving metallic sodium, amorphous boron powder, and titanium tetrachloride at 400°C within an autoclave. Including benzene as a reaction medium regulated the reaction rate and particle size [34]. Lu et al. [35] used microwave CVD to deposit TiB_2 films on a graphite substrate. They found that increasing microwave power and deposition temperature improved the micro-hardness, grain size, and growth rate of the TiB_2 film, ultimately leading to the production of bulk TiB_2 with increased hardness. As shown in Figure 4a, the microwave heating CVD system was used to deposit TiB_2 films, and XRD patterns indicated that increasing power led to a change in the crystal structure of the movie. SEM micrographs revealed the TiB_2 films had a uniform microstructure.

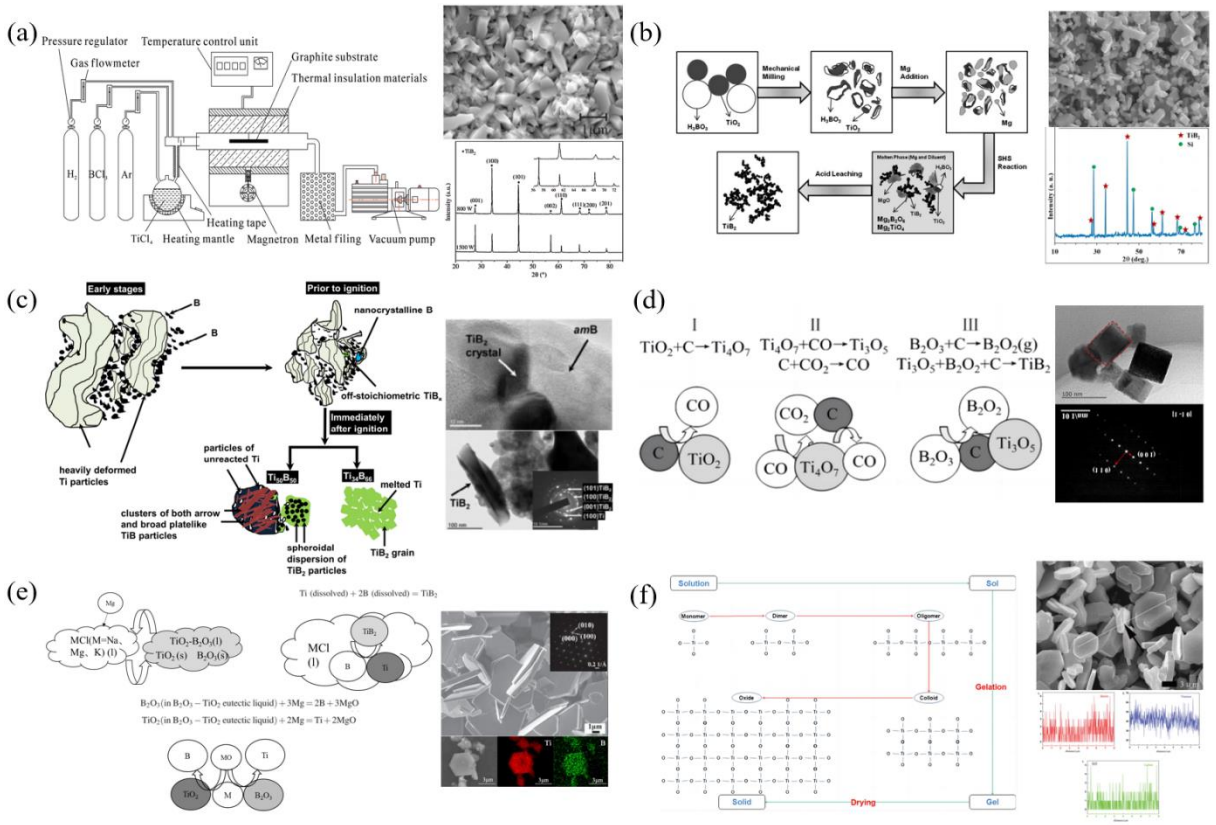

Figure 4 Reaction mechanism and microstructure of TiB_2 powder synthesis: (a) gas phase method [35]; (b) SHS method [36, 37]; (c) High energy ball-milling method [38]; (d) Carbon thermal reduction method [39]; (e) MSS method [40, 41]; (f) Sol-gel method [42].

3.2 Solid Phase Method

The existing commercial TiB_2 is mainly obtained through the solid phase method. The commonly used solid phase methods include the direct synthesis method [38], self-propagating high-temperature synthesis method [43], high-energy ball milling method [44], carbothermal reduction method [45], boron thermal reduction method [46], boron/carbothermic method Reduction method [47], metal thermal reduction method [48], etc. For the direct synthesis method, although the purity of the powder obtained is high, the temperature used is high, the particle size of the obtained product is large, and the activity is low, which is not conducive to subsequent sintering. In addition, to produce high-quality TiB_2 powders, the reaction must be carried out in an inert or reducing atmosphere to minimize the formation of oxide impurities. The relatively high cost and low production capacity greatly limit the commercial application of this method. Therefore, the preparation methods of TiB_2 powders based on reduction reaction are only introduced.

3.2.1 Self-Propagating High-Temperature Synthesis Method

The self-propagating high-temperature synthesis process (SHS) uses the heat energy the combustion reaction releases to sustain the reaction. It has the characteristics of internal heat release and fast combustion speed. Once the response is ignited, it can reach incredibly high temperatures

Quickly. For example, Ipekçi [49] et al. prepared sub-micron TiB_2 powder via the SHS process using TiO_2-B_2O_3-Mg powders as the starting materials. The resulting MgO, $Mg_3(BO_3)_2$, and Mg by-products could be leached using hydrochloric acid. The SHS diluents are expected to control the particle sizes and shapes. Khanra [50] et al. found that as the addition of NaCl diluent increased to 20 wt.%, the particle size of TiB_2 gradually decreased to ~26 nm. Nozari [36] et al. used TiO_2, H_3BO_3, and Mg powder as raw materials to prepare TiB_2 powder using the SHS process and studied the effect of mechanical alloy assistance on the phase composition and morphologies. Liu [37] used the SHS process to develop TiB_2-Si ceramic-metalloid powder feedstocks for SLM of ceramic-based composite. The scanning electron microscope (SEM) images and the XRD pattern of porous bulk TiB_2-Si products produced by SHS are shown in Figure 4b, revealing the presence of hexagonal titanium diboride and no spurious phase formation [36, 37]. However, SHS technology also has some drawbacks: the reaction process is usually accompanied by higher heating and cooling rates, increasing the concentration of TiB_2 defects.

3.2.2 High-Energy Ball Milling Method

High-energy ball milling (HEBM) is designed as an intermediate step to promote reactions, including mechanochemical reactions and mechanical activation. It is a valuable and straightforward method for preparing nanocrystalline TiB_2 powders and other composites. For example, Tang [51] et al. used Ti-67B elementary powders and found that the diffusion-reaction mechanism controlled the formation of TiB_2 nanocrystals. At the beginning of ball milling, Ti(B) solid solution was first formed, then Ti(B) changed from amorphous to crystalline. Finally, pure-phase nanocrystalline TiB_2 is formed. Titanium diboride can also be produced by ball-milling a mixture of TiO_2, B_2O_3, and Mg [44]. The milling process facilitated the completion of the reaction without any detectable residual Mg, while the undesired phase, MgO, was effectively eliminated through acid leaching. Ricceri et al

obtained the nanometric TiB_2 (about 50-100 nm) powders by high-energy ball milling of easily available powders like B_2O_3, TiO_2, and Mg [52]. Kim and co-workers used the mechanochemical reaction between $LiBH_4$, LiH, and $TiCl_3$ by high-energy ball milling to produce TiB_2 particles dispersed within a soluble LiCl matrix. The process resulted in TiB_2 nanopowders ranging from 15-60 nm in particle size, achieved through successive washing steps with distilled water, ethanol, and acetone to eliminate the LiCl matrix phase [53]. Nozari [36] et al. synthesized TiB_2 through a milling-assisted self-propagating high-temperature synthesis (MA-SHS) approach employing TiO_2. The energy required to initiate SHS decreased compared to unmilled powders through mechanical activation on the initial powder mixture. Rabiezadeh [54] et al. used a sol-gel-assisted mechanical alloying method to prepare TiB_2 powder with a 20-40 nm particle size using TTIP, B_2O_3, and Al as the starting precursors. Oghenevweta [38] et al. explored the mechanically induced self-propagating reaction synthesis of titanium boride and diboride using elemental mixtures of titanium and amorphous boron. Figure 4c shows the reaction mechanism, and the SAD pattern in Figure 4c shows diffraction spotty rings or spots corresponding to Ti and TiB_2, along with additional diffuse contrast that can be attributed to amorphous boron. In conclusion, HEBM can be used for mechanical activation of the powders before sintering to lower sintering temperature, shorter holding time, and maintain ultra-fine size.

3.2.3 Reduction Methods

The reduction process is possibly the most commonly adopted approach. It includes carbothermic, boron thermal reduction, carbon/boron thermal reduction, and metallothermic reduction (aluminothermic reduction, magnesiothermic reduction, and silicothermic reduction). The reaction mechanisms for these reactions are summarized in Table 2.

Table 2 The primary reactions of TiB_2 powder synthesis.

Reaction Type	Reaction equations	No.
Carbothermic reduction reaction [55]	$TiO_2 + B_2O_3 + 5C = TiB_2 + 5CO$ (g)	(1)
Boron reduction reaction [46]	$TiO_2 + 4B = TiB_2 + B_2O_2$ (g)	(2)
Boron/carbide reduction reaction [40, 56]	$TiO_2 + 5/7B_4C = TiB_2 + 5/7CO$ (g) + $3/7B_2O_3$	(3)
	$TiO_2 + 1/2B_4C + 3/2C = TiB_2 + 2CO$ (g)	(4)
Metallothermic reduction [57]	$TiO_2 + B_2O_3$ + M (Mg, Al, Si) → TiB_2 + MO (MgO, Al_2O_3, SiO_2)	(5)
$NaBH_4$ reduction method [32]	$TiCl_4 + 2NaBH_4 = TiB_2 + 2NaCl + 2HCl + 3H_2$	(6)

Carbothermic Reduction Reaction. In the TiB_2 powder synthesis technology, the carbothermic reduction method is simple and commonly used. It does not require a complicated manufacturing process and can produce TiB_2 powders industrially. In Figure 4d, submicron-sized TiB_2 particles (100-400 nm) exhibit hexagonal short-column morphologies, displaying excellent dispersion. These particles were identified as single crystalline TiB_2 through SAED and XRD analysis [39]. To study the influence of raw precursor materials on the synthesis of TiB_2 powders, Yu [55] et al. studied the impact of different boron sources (B_2O_3, H_3BO_3, and HBO_2) on the microstructure and final phase formation of TiB_2 at different carbothermal temperatures. Under the optimal conditions of 1700°C, pure-phase TiB_2 powders with a grain size of ~10.0 μm were obtained. Sahoo [58] et al. found that

adding 10 wt.% of carbon source under thermal plasma can achieve better powder yields. Bahrami [59] et al. studied the influence of the reactants' stoichiometric ratio on the product's phase composition, considering that the volatilization of the boron source at high temperatures led to insufficient reaction. Although this can be compensated by introducing an excessive amount of boron source, the loss of boron source cannot be calculated due to the unpredictability of volatilization, and the final product will inevitably contain impurities such as carbides. Generally speaking, the carbothermic reduction process is a solid exothermic reaction with a long reaction period. During this process, the growth of TiB_2 grains and the adhesion of individual grains will occur. Therefore, the optimization of the carbothermic reduction process is continuing.

Boron Reduction Reaction. The boron thermal reduction method is a process in which elemental boron is used to reduce TiO_2 to obtain TiB_2 and gaseous B_2O_3. Compared with the carbothermic reduction method, the appearance of carbide impurities can be avoided due to the excessive amount of boron source. For example, Guo [46] et al. discussed the process of boron thermal reduction of TiO_2 under vacuum conditions, and the results showed that with the increase of temperature, TiO_2 was first reduced by boron to produce $TiBO_3$ and Ti_2O_3, and then TiB_2 and B_2O_3. Although the by-product B_2O_3 can be removed by high-temperature evaporation or the formation of gaseous boron-rich oxide, it is still considered the most critical factor in promoting particle coarsening. Recently, a low-temperature molten salt-assisted synthesis technology has been proposed to lower the reaction temperature. On this basis, Liu [60] et al. used KCl/NaCl mixed molten salt assisted boron thermal reduction technology to successfully synthesize high-purity ultrafine TiB_2 nanopowders at a relatively low temperature of 900°C. However, because the by-product B_2O_3 is challenging to remove at low temperatures, the oxygen content in the synthesized powder is relatively high. It is concluded that this will not be conducive to improving the mechanical properties of TiB_2-based ceramics.

Boron/Carbothermic Reduction Reaction. Because of the stability of B_4C at high temperatures, people have been actively researching the synthesis of TiB_2 powders by the boron/carbothermic reduction method since the last century. For example, Yu [56] et al. used TiO_2, B_4C, and C as raw materials. They directly synthesized TiB_2 powders with an average particle size of 0.5 to 1.0 μm using the boron/carbothermal reduction method at 1600°C for 30 min. Krutskii [61] et al. used B_4C and nanofiber carbon to reduce TiO_2 under argon protection to prepare TiB_2 powders with an average particle size of 7.4~8.0 μm. The powders were mainly aggregated and contained a small amount of impurities. Subramanian [62] et al. used TiO_2, B_4C, and petroleum coke as raw materials and synthesized fine TiB_2 powder with a particle size of about 0.8 μm at 1800°C using boron/carbothermic reduction technology. Ma [63] et al. prepared sub-micron TiB_2 powders using the boron/carbothermic reduction method by selecting the appropriate reaction temperature and raw materials. As shown in Figure 4e, at a temperature of 1300°C, rapid growth of the layer occurs, and nucleation on the surface is suppressed during the preparation of sub-micron TiB_2 powders via the SHS process using TiO_2-B_2O_3-Mg powders, according to Liu [40] et al. Some researchers have also used the MSS method to prepare TiB_2, the schematic diagram of which is shown in Figure 4e, and it also discovered when the temperature increases to 1300°C, the layer proliferates, and the nucleation on the surface is suppressed [41]. However, the above results show that the

boron/carbothermal reduction process requires a very high synthesis temperature and high synthesis conditions, significantly limiting its wide application.

Metallothermic Reduction. The metal thermal reduction method is a method in which metal is used as a reducing agent to prepare TiB_2 powder. The thermal reduction of metals, especially magnesium, shows significant advantages in reducing the reaction temperature. In addition, magnesium as a reducing agent can acid-leach unwanted by-products and release TiB_2 powders. However, the thermal reduction process of magnesium also has its shortcomings. Because it usually releases a large amount of heat in a short time, the reaction process can be completed in a short time, making it difficult to effectively control and further particle agglomeration. It is often necessary to introduce molten salt into the reaction system to slow down the reaction rate. For example, Bao [57] et al. used TiO_2, B_2O_3, and Mg as raw materials and $KCl/NaCl/MgCl_2$ as mixed molten salt to synthesize particles at 1000°C. However, due to the volatility of magnesium and the complexity of chemical reactions in the thermal reduction of magnesium, it is still challenging to prepare high-purity TiB_2 powders.

$NaBH_4$ Reduction Method. To effectively reduce the particle size of the synthetic powder, the sodium borohydride reduction method was developed based on the above-mentioned synthetic method. For example, to synthesize nanocrystalline TiB_2 powder, Chen [32] et al. mixed titanium chloride and sodium borohydride in an autoclave at 500-700°C to prepare nanocrystalline TiB_2 with a particle size of about 10-20 nm. Although this method can synthesize TiB_2 powder at a very low temperature, sodium borohydride as a raw material harms the human body and the environment, limiting the popularization and application of this method.

As a result, the above five reduction methods have different advantages and disadvantages in preparing the TiB_2 powders. The carbothermic reduction method is widely used to prepare the TiB_2 powders, but some carbide impurities can not be removed, affecting the purity of the powders. For the boron reduction method, the by-product B_2O_3 formed during the reaction is difficult to remove, leading to the high oxygen content in the synthesized powders. Further, the boron/carbothermic reduction reaction method is beneficial for synthesizing powders with high quality by covering the shortages of the above two methods. However, in comparison, a high synthesizing temperature is needed to promote the reaction. Metallothermic reduction can synthesize TiB_2 powders at low temperatures by introducing molten salt and magnesium. Still, some impurities can inevitably be introduced in powders, affecting the quality of powders. The $naBH_4$ reduction method is beneficial for preparing the nanopowders, but the used materials are not environmentally friendly. Therefore, newly developed methods are still urgent in improving the powders with high quality.

3.3 Liquid Phase Method

Many inorganic materials can be prepared by simply mixing reactant powders. Although the reaction conditions are relatively easy to achieve, they are also limited by the uniform mixing of raw materials. In a mixture of two or more, the initial reaction occurs at the edges of adjacent particles. If the diffusion of the reactants is hindered, unreacted areas will be found. Although some of these problems can be overcome by ball milling with optimized parameters, it makes the process more cumbersome.

The liquid phase method, such as the sol-gel technique, is a more versatile synthesis route capable of addressing various challenges. In contrast to conventional synthetic approaches, the sol-gel method is a promising means for low-temperature synthesis of fine powders. Additionally, employing the sol-gel method offers the advantage of achieving high chemical and phase homogeneity by thoroughly mixing the initial components at either the molecular or colloidal level. The powders synthesized by this method have a relatively small particle size [42, 64]. Figure 4f shows the schematic diagram of the sol-gel process, the EDS line scanning of TiB_2 powder particles, and the total boron, titanium, and carbon records. Zhang [65] et al. devised a synthetic process wherein ultrafine TiB_2 was produced through a sol-gel approach combined with a microwave-assisted carbothermal reduction process, employing tetrabutyl titanate, boric acid, and sucrose as precursor materials. Their study revealed that the primary factors influencing the synthesis of ultrafine TiB_2 powder were the formulation of materials and the temperature employed in the process.

3.4 Controlled Synthesis of Anisotropic Particles

It is determined that the anisotropic particles can be obtained in some conditions owing to the inherent properties of TiB_2. Carlsson [66] et al. synthesized TiB_2 whiskers at 1500°C using a V-L-S (vapor-liquid-solid) growth mechanism through a carbothermal reaction. During the response, the B source and Ti source directly form the gas phase, and they will dissolve into a liquid phase formed by a catalyst at high temperature under the function of flowing gas (Ar + H_2). When the supersaturation of the reaction in the liquid phase is formed, the reaction molecules will precipitate from the liquid phase to create the whiskers. The obtained whiskers have a diameter of 0.5-2 μm and a length of 10-50 μm. In the VLS growth mechanism, molten and Ni/Co/Fe are liquid catalysts. Ti and B sources are transported to liquid metal droplets as gaseous chlorides. In addition, Krishnarao [67] found that K_2CO_3 can react with TiO_2 to form a low-melting liquid when synthesizing TiB_2 whiskers, while $NiCl_2$ can catalyze carbon gasification. Both can assist in the formation of whiskers through the V-L-S growth mechanism.

The current literature on the preparation of two-dimensional TiB_2 powder is mainly focused on the research of hexagonal flake TiB_2 powders, which is also consistent with the hexagonal structure characteristics of TiB_2. Yu et al. [55] successfully prepared TiB_2 powder using TiO_2, HBO_2 and C as raw materials by carbothermal reduction. The synthesized hexagonal pure TiB_2 particles with a size of about 10.0 μm were obtained at 1700°C for 30 minutes. Hu [68] et al. synthesized TiC-TiB_2 composite powders using titanium dioxide, boric acid, and different carbon sources through a carbothermal reduction method. The study found that carbon black was beneficial for producing TiC, while sucrose and glucose were beneficial for producing TiB_2. The powders synthesized using carbon black had the most minuscule particles with approximately 100 nm, and increasing the amount of boric acid led to a change in morphology towards less spherical particles with irregular structures. Liu et al. [40] successfully synthesized hexagonal TiB_2 with an average size of about 4.5 μm at 1200°C under microwave heating by a molten salt-assisted carbothermic method using TiO_2, B_4C, and C as raw materials.

In addition, due to the randomness of the solution state, the mixing of the raw materials at the molecular level is ensured to produce solid materials from chemically homogeneous precursors and control particle morphology. Bača et al. successfully prepared low-cost titanium diboride (TiB_2) powders by sol-gel process. The hexagonal plate-like TiB_2 grains with a particle size of about 2 μm

and thickness of 200 nm were obtained by carbothermal reduction at 1300°C for 1 h [69]. Zhang et al. [65] synthesized hexagonal TiB_2 sheets with a size of 2-4 μm at 1100°C via sol-gel and microwave carbothermic methods using tetrabutyl titanate, sucrose, and boric acid as raw materials. However, at this temperature, the purity of TiB_2 was not high and contained a large amount of unreacted reactants. With the temperature increase, the hexagonal TiB_2 flakes were finally transformed into 3-5 μm particles at 1300°C. Song et al. [41] synthesized a hexagonal TiB_2 plate with a side length of 3-8 μm and a thickness of 200-500 nm at 1300°C for two h by a molten salt-assisted sol-gel carbothermic method using tetra butyl titanate, sucrose, and sodium borate as raw materials. And the author found that the growth of hexagonal TiB_2 plates on the side showed a dot-line-plane growth trend by controlling the holding time and thus forming hexagonal TiB_2 plates, indicating that its growth was conformed to be the surface adsorption growth model.

Finding a simple and environmentally friendly synthesis method for TiB_2 has always been the goal of scientific researchers. It can be seen from the above analysis that a single method can no longer meet the current production needs, and the combination of multiple methods has become a trend. Especially for preparing ultrafine and anisotropic powders, the combination of sol-gel and molten salt method has shown substantial advantages and will become a hot spot.

4. Sintering Methods of TiB_2-Based Ceramics

It is challenging to realize the densification of TiB_2 ceramics due to the strong covalent bonding, very high melting points, low self-diffusion coefficient, and existing oxide layer or other impurity on the surface of powders [4, 9, 27, 70]. Therefore, achieving fairly dense monolithic TiB_2 ceramics during sintering, particularly when employing the conventional pressureless sintering method, necessitates high sintering temperatures. While near-theoretical sinter-densities can be attained at these elevated sintering temperatures, substantial grain growth often occurs, adversely impacting the mechanical properties. Achieving sintered bulk ceramics characterized by both high sinter-density and fine grain size concurrently poses a significant challenge, mainly when high sintering temperatures are essential. Consequently, optimizing the sintering process and its associated parameters is a critical factor in addressing this challenge [71].

This section encompasses a discussion on commonly employed sintering techniques, encompassing both traditional methodologies like pressureless sintering, hot-pressing sintering, and reaction processing, as well as more advanced approaches like spark plasma sintering, flash sintering, laser sintering, reactive sintering, and microwave sintering. In short, the advantages and disadvantages of these sintering technologies are briefly described in this section.

4.1 Traditional Sintering Methods

Pressureless sintering (PS), as shown in Figure 5a, the scheme of the liquid phase sintering mechanisms upon heating is illustrated [72], which enables the fabrication of components to near-net shape using standard powders, is possibly the most straightforward and commonly used sintering technique compared to the more advanced sintering techniques [4, 27]. In the PS process, the initial powders, supplemented with sintering additives if necessary, are blended in suitable proportions. These mixtures are then cold-pressed within a die at pressures ranging from about 100-400 MPa to form the desired compact shape. Subsequently, sintering is carried out at temperatures typically exceeding 70% of the absolute melting temperature to facilitate

densification. Typically, achieving high sinter density in titanium diboride through the PS technique requires sintering temperatures of 2000-2300°C.

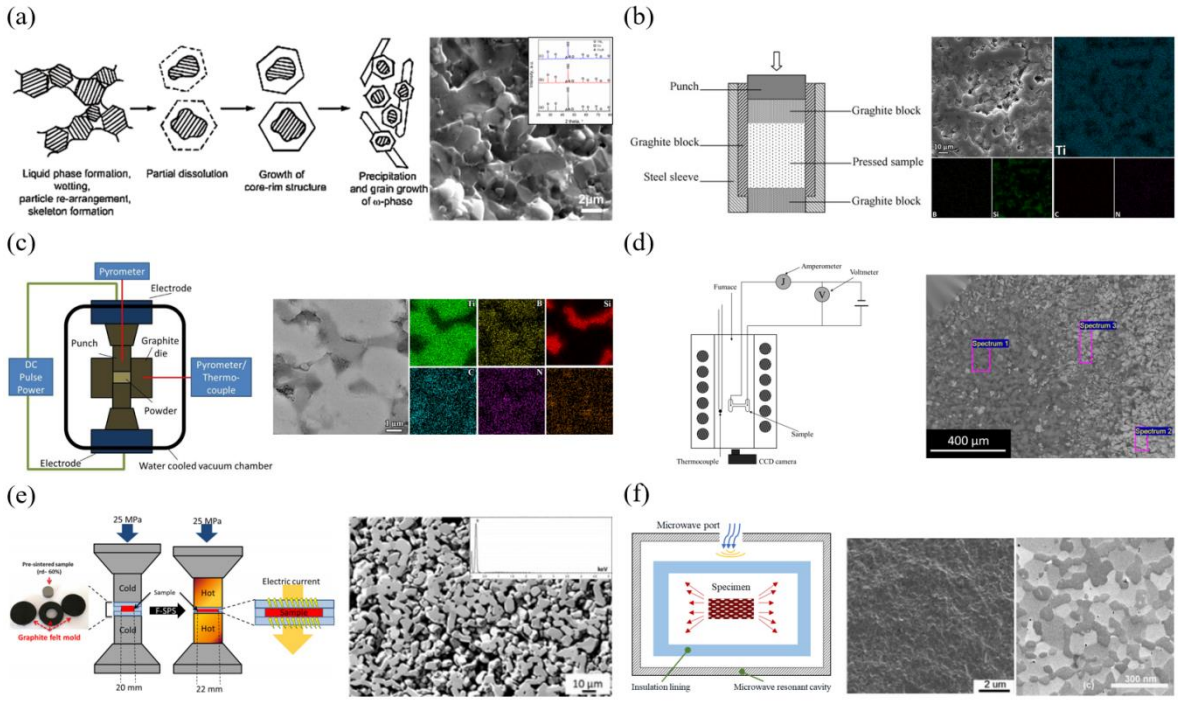

Figure 5 Reaction mechanism and microstructure of different sintering methods for TiB_2: (a) Pressureless sintering [72, 73]; (b) Hot-pressure sintering [74]; (c) SPS method [75, 76]; (d) FS method [77]; (e) FSPS method [78]; (f) Microwave sintering method [79].

Baumgartner and Steiger obtained the pure TiB_2 powders with submicron size, and the near theoretical density of monolithic TiB_2 ceramics was prepared by using PS method [80]. The density of TiB_2 prepared at 2000°C for 1 hour was almost close to the theoretical sinter density. However, when the sintering temperature exceeded 2100°C, the abnormal grains began to grow with the increase of holding time, and the mechanical properties decreased rapidly. It was reported that $MoSi_2$ (up to 25 wt.%) was used as a sintering additive for TiB_2, and inferior densification was achieved (~90% ρ_{th}) even after PS at 1900°C for 2 h [4]. Indeed, in the sintering of TiB_2, high sintering temperatures and the utilization of highly pure and finer starting powders are crucial factors contributing to the attainment of excellent sinter density. Some researchers also use the method of liquid phase sintering without pressure to densify the TiB_2 ceramics [73]. For example, metals can also be used as the sintering additive to densify the TiB_2 ceramics. It was reported that densified titanium diboride ceramics containing 0.5 wt.% Cr and 0.5 wt.% Fe was obtained by pressureless sintering at 1900°C [81]. As shown in Figure 5a, for the sintered TiB_2-3Co sample, the facture morphology showed the densification behavior.

In general, achieving near-theoretical sinter-density of titanium diboride involves two predominant approaches: pressureless sintering at high temperatures exceeding 2000°C and the addition of sintering additives at comparatively lower sintering temperatures. However, a key challenge associated with pressureless sintering is the necessity for high temperatures, which can result in the melting or vaporization of components with lower melting points. This elevated temperature can also induce microstructural coarsening and abnormal grain growth, presenting

significant drawbacks. Further, it will lead to micro-cracking at the grain boundaries, detrimental to the mechanical and thermophysical properties.

Hot pressing (HP) sintering applies a uniaxial pressure (typically 20-50 MPa) to powder mixtures and temperature to obtain a dense body. Figure 5b shows the schematic illustration of hot-pressing sintering. The TiB_2 composites by hot pressing have improved mechanical and thermal properties due to the fine-grained and denser microstructures than those by PS samples. It was reported that TiB_2 could be densified via PS at 2000°C, whereas it required only 1800°C via HP [80, 82]. Subramanian and co-workers prepared the titanium diboride powders by carbothermic reduction and then densified them by HP at 1800°C [62]. The TiB_2 ceramics with a high density of 97.56% ρ_{th}, hardness of 26 GPa, and fracture toughness of 5.3 MPa $m^{1/2}$ were successfully prepared. Wang [71] et al. investigated the influence of hot-pressing temperature and duration on both the densification behavior and mechanical properties of titanium diboride. Sintering temperature and time obviously influence the density and grain growth of TiB_2 ceramics. The density of the samples increased rapidly at first and then gradually leveled off, which indicated that the sintering mechanism was different in different sintering stages. The grain size of TiB_2 demonstrated an increase with prolonged sintering duration, particularly noticeable at 1800°C. The polished surface of the powder mixture of TiB_2, SiC, and TiN samples, along with the relevant EDS map results, are shown in Figure 5b [74]. Therefore, in terms of hot-pressing sintering, optimizing sintering parameters dramatically influences the density of TiB_2.

Compared with PS, TiB_2 ceramics can be obtained by hot pressing sintering at lower temperatures. However, a disadvantage of this process is that complex shapes (limited to disks and bars) cannot be prepared due to the uni-axial load application. Additionally, it's crucial to note that even with pressure-assisted sintering techniques, pure monolithic TiB2 could not achieve complete densification under such conditions.

Reaction Processing (RP) is another route to produce TiB_2 ceramics with low impurity content and high sintering density, which can be carried out at a relatively low temperature. This process involves the in-situ formation of TiB_2 via chemical reactions between Ti (or TiH_2) and boron source (B or B_4C) to form a solid body. Indeed, when reactive processing occurs under pressure, it's termed reactive hot pressing (RHP). However, if the process is conducted without applying pressure, reaction sintering (RS) [65, 83, 84]. Processing TiB_2 is highly advantageous due to its inherent characteristics. The reaction involved during processing tends to be highly exothermic, leading to locally generated elevated temperatures that significantly enhance the reaction rate. Additionally, RP is also advantageous for the improvement of properties for TiB_2 since the interfaces among the phases in the final product are usually clean, and the grain sizes are relatively delicate and more uniform. Zhang et al. developed a TiB_2-SiC composite using TiH_2, Si, and B_4C according to the equation (1) [85]. It was observed that while transient phases like TiC and Ti_5Si_3 were present in the initial stages of the reaction, the conclusive phases formed at 1350°C comprised solely TiB_2 and SiC. Furthermore, the TiB_2-SiC composite with a bending strength of 332 MPa and fracture toughness of 8.67 MPa $m^{1/2}$ has been produced by reactive hot pressing at 2000°C under 30 MPa for 60 min in an Ar atmosphere.

$$\mathrm{Si} + 2\mathrm{TiH_2} + \mathrm{B_4C} \rightarrow \mathrm{SiC} + 2\mathrm{TiB_2} + 2\mathrm{H_2} \quad (1)$$

In another work, high-density TiB_2-TiC composites have been successfully synthesized using in situ reaction of B_4C and Ti powder mixtures at relatively high temperatures. The samples did not identify transient phases (Ti_3B_4, TiB, Ti_2B_5) and free Ti phases [40]. TiB_2-SiC ceramic composites were in-situ synthesized by the reactive hot pressing (RHP) process at 1700°C under 32 MPa in a vacuum [55]. The composition, as determined by X-ray diffraction (XRD), revealed a complete conversion of reagents into products. Additionally, the addition of SiC significantly affects the composites' microstructure and mechanical properties.

TiB_2 composites, such as TiB_2-SiC and TiB_2-TiC, stand as appealing structural materials owing to their distinctive amalgamation of high melting temperatures, low density, exceptional thermal and chemical stability, outstanding wear resistance, and high fracture toughness. In summary, both reactive pressing (RP) and reactive hot pressing (RHP) are promising in-situ preparation techniques, enabling the direct in-situ synthesis of secondary phases within the ceramic matrix. Moreover, the literature on high-temperature properties of the developed TiB2 via RP or RHP is relatively sparse and needs further research.

4.2 Advanced Sintering Methods

Spark Plasma Sintering (SPS) is an advanced technique in which ceramic powders can be sintered rapidly to total density by the direct electric current via the electrodes at the top and bottom punches of the conducting graphite die. SPS's rapid heating rates (hundreds of °C/min), which can minimize coarsening and facilitate rapid densification, is highly suitable for acquiring dense TiB_2 [41, 68, 86-88]. Figure 5c shows the schematic of the spark plasma sintering method [75].

The effects of sintering parameters (sintering temperature, sintering pressure, and pressure method) on the mechanical properties and densification of TiB_2 ceramics have been studied [89]. It can be noted that the sintering temperature has a great influence on the relative density and microhardness of TiB_2. As the sintering temperature surpasses 1700°C, there's a rapid escalation in the relative density. However, the microhardness of TiB_2 ceramics demonstrates a more gradual increase under these conditions. TiB_2 ceramic during SPS has a slow grain growth rate and finally forms fine grains. The main reason was attributed to the fast sintering speed and the low temperature required during SPS, which effectively prevents the growth of grains.

However, the issue of non-uniform densification and properties arises mainly from rapid heating rates and shorter holding times. To tackle this challenge, a solution has been proposed: the design of a multi-stage spark plasma sintering (MSS-SPS) schedule. This schedule involves holding at one or more intermediate temperatures for a few minutes before reaching the final sintering temperatures [90-92]. It has been reported that more uniform densification and finer microstructures were achieved for TiB_2-$TiSi_2$ composites by MSS-SPS [93]. More recently, the RP and FAST have been combined with SPS for densification and sintering of TiB_2. Reactive processing adopted for SPS was known as reactive spark plasma sintering (RSPS). In analogy with reactive hot pressing, the monolithic TiB_2 was synthesized at a low temperature [94]. The material initially displayed favorable mechanical properties. However, with an increase in the TiB phase content, there was a subsequent decline in the material's mechanical properties. Balcı [95] et al. successfully achieved high-density TiB_2 ceramics at reduced temperatures (1500°C) by employing field-assisted sintering technology, specifically the spark plasma sintering (FAST/SPS) technique. The TiB_2 ceramics fabricated via SPS at 1500°C under 60 MPa pressure yielded elongated grains with an average size

of 6μm, achieving a relative density of 96.7%. The additional pressure field efficiently obtained very dense TiB_2 ceramics at a lower temperature. Based on the EDS map analysis (Figure 5c), the phases distinguished by light-gray and dark-gray coloring are likely attributed to the SiC reinforcement and in-situ formed TiC [76].

Overall, SPS is superior to the other conventional techniques in improving the densification and mechanical properties of TiB_2. Future efforts should primarily optimize the sintering parameters within the multi-stage SPS process. This optimization aims to control any undesired sintering reactions that might adversely impact the properties of the resulting sintered ceramics or composites.

Flash sintering (FS) (Figure 5d) [77] is a novel sintering technique that enables rapid densification of ceramics at low temperatures and short processing times. During FS, an electric field is applied to the ceramic powders, rapidly heating the material to high temperatures at a constant rate. When the furnace temperature is low, the ceramic materials have a low resistivity and low current. With increasing furnace temperature, the current increases gradually. When the furnace temperature reaches the critical temperature, the resistivity of ceramics decreases suddenly, and the current increases essentially, leading to the realization of flash sintering. The heating process is completed in a matter of seconds, much faster than traditional sintering methods, which can take hours or even days [96].

As shown in Figure 5e [78], flash spark plasma sintering (FSPS), the combination of FS and SPS, was first proposed and proved feasible by Grasso et al [97]. The central areas are incredibly dense for the sample sintered by FSPS, but the rim areas are less thick. It replaces the FS platinum electrode with an inexpensive graphite one, and the samples with a large (Ø ≈ 10 cm) diameter can be prepared using a low voltage (<10 V). Furthermore, it eliminates the need to preheat the samples using partially sintered green compaction instead of powders. Moreover, the graphite die used in the SPS was removed, reducing energy consumption and providing convenience for automated use [98]. So far, it has been confirmed that FSPS can be used to attain high densities in a very short time (<1 min) for TiB_2 [78]. McKinnon and co-workers reported that nearly dense (up to 97%), crack-free discs of TiB_2-hBN (Ø 35 mm) had been flash sintered directly from cold-pressed green bodies using a die-less FSPS configuration for the first time [99]. It was observed that removing graphite dies from the field-assisted spark plasma sintering (FSPS) setup led to the development of texture in sintered samples, characterized by h-BN plate-like grains aligned perpendicular to the cold-pressing axis. Recently, a method involved pre-sintering pure TiB_2 ceramic using conventional SPS, followed by consolidation via FSPS without dies, achieving this within 20 or 40 seconds [78]. It was revealed that the relative density was up to 98.3% in the central areas of the specimens.

Indeed, microwave sintering represents an alternative sintering method with distinct advantages. One key benefit is the absence of a requirement for external pressure during the sintering process. Moreover, it offers advantages such as uniform (at the molecular level) and swift heating, achieved through the intrinsic interaction of microwaves with the material. This method is characterized by higher energy efficiency as heat generation occurs internally within the sample due to the interaction of microwaves with the material [100, 101]. Dense TiB_2 ceramics (RD: 98.5%) have been produced by microwave sintering at 1700°C for 30 min under a controlled atmosphere [102] (Figure 5f). It was found that a uniform microstructure and normal grain growth existed at high temperatures due to microwave sintering. In another work, the highly dense TiB_2 ceramics (RD: 99%) with the uniform crack-free microstructure were produced by microwave sintering at 1650°C for 10

min with the addition of TiN [79] (Figure 5f). The addition of TiN to the TiB_2 ceramics allows for highly homogeneous heating during microwave sintering of the composite, resulting in the retainment of a fine-grain structure.

As mentioned in the above sections, various sintering techniques have been successfully used to realize the densification of TiB_2 ceramics. The research focusing on the sintering and densification of TiB_2 ceramics has shifted from traditional (such as PS, HP) to advanced (such as SPS, FSPS). Especially in the research on the SPS method, it has been found that using a multistage SPS scheme can make the microstructure of diboride ceramics more uniform. Optimizing the sintering parameters within multi-stage SPS will be crucial for controlling any undesired reactions that might potentially impact the properties of the resulting sintered material. This focus on parameter optimization is vital for enhancing the overall quality and performance of the sintered material. In addition, new sintering technologies should also be developed to prepare the densified TiB_2 ceramics or composites.

5. Densification, Microstructural Control and Mechanical Properties

The mechanical properties of ceramic materials are directly related to their components and microstructure. To control the densification and microstructure of TiB_2-based ceramics, the primary methods include the introduction of sintering additives, the second phase, and the texturing process et al. This section will focus on controlling the densification and structure of TiB_2-based ceramics and improving mechanical properties by these methods.

5.1 Sintering Additives

Appropriate sintering additives play an essential role in the densification of TiB_2 ceramics, which can reduce the sintering temperature and inhibit grain growth. Meanwhile, it is necessary to consider whether the sintering additives will react with TiB_2. There are usually two kinds of sintering additives: metal and non-metal sintering additives. Metallic sintering additives such as Ni, Co, and Fe are often used to densify TiB_2. Non-metallic sintering additives, including some carbides (SiC, B_4C, TaC), silicides ($MoSi_2$, $TiSi_2$), nitrides (TiN, AlN, Si_3N_4), and borides (CrB_2) et al are often used to improve the sinterability and the mechanical properties of TiB_2 ceramics. The influence of metal and non-metal sintering additives on the densification, microstructure, and mechanical properties of TiB_2 are introduced in the following sections.

5.1.1 Metallic Sintering Additives

The selection of metal sintering additives is usually needed to consider its wettability with matrix (TiB_2). It has been reported that Ni, Co, and Fe are commonly usually used as sintering additives for their good wettability with TiB_2 [103-105]. Since then, many researchers have used several metal sintering additives and optimized sintering conditions to improve the sinterability and mechanical properties of TiB_2. In this process, various metal sintering additives are considered to be capable of sintering TiB_2 at lower temperatures. The use of metallic additives such as nickel, iron, cobalt, stainless steel, and manganese has demonstrated that 99% of ρ_{th} can be achieved by liquid phase sintering (LPS) during the sintering process [106, 107]. The microstructures observed in bulk TiB_2 produced via liquid phase sintering (LPS) utilizing metals as additives resemble those found in other

hard metals such as WC-Co. Ferber [107] et al. have obtained the TiB_2 composites with a theoretical density of 99% by adding 10% Ni under hot pressing at 1425°C. Reportedly, the density achieved for samples containing 1.5 wt.% of nickel, sintered at 1500°C in an argon atmosphere, reached as high as 95% of the theoretical density. This density approximated the levels obtained for hot-pressed TiB_2 ceramics [108]. Researchers have discovered that adding Mo has a dual effect: it reduces the highest combustion temperature and enhances the compatibility between the binder and TiB_2. As a result, this addition diminishes the cermet's porosity and reduces the ceramic particles' size [109]. The fractured surfaces and strengthening mechanism for TiB_2-Ti(C,N)-Ni cermet without Mo and with Mo addition are shown in Figure 6a. Fu et al. [73] (Figure 6b) found that the addition of 3 wt.% Co was sufficient to facilitate the densification of TiB_2 and maintain a delicate and homogeneous structure. Figure 6c reveals that nickel mainly exists at the grain boundaries, where it forms a thin film (A) which links the TiB_2 grains, but it is also present in the form of larger agglomerates (B) [110].

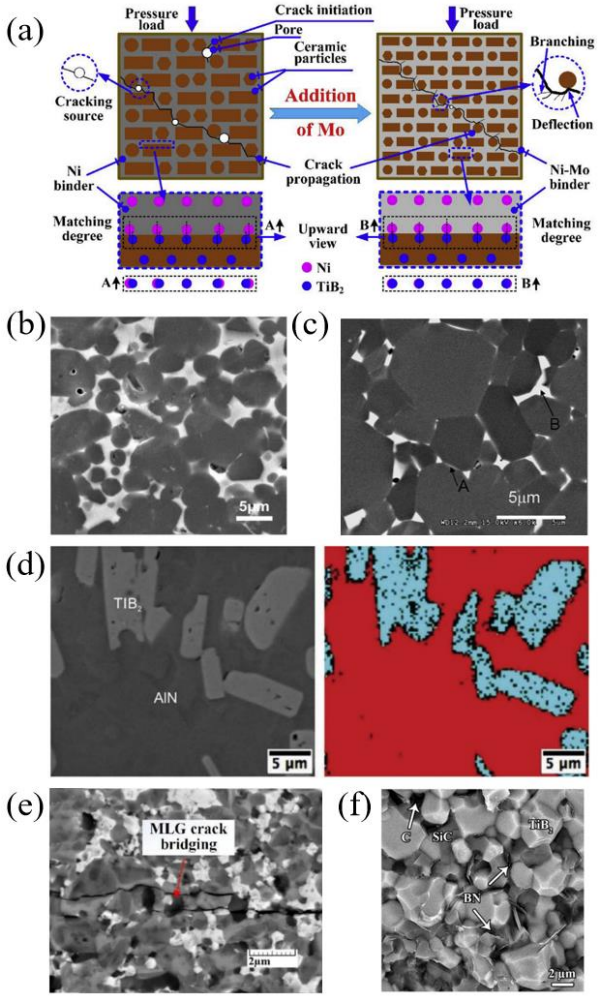

Figure 6 The densification microstructure and mechanism of different sintering aids for TiB_2: (a) Strengthening mechanism for TiB_2-Ti(C,N)-Ni cermets [109]; (b) SEM microstructure of TiB_2 sintered with 20 wt.% Co at 1500°C [73]; (c) SEM micrograph of TiB_2/Ni composites [110]; (d) Scanning electron microscopy (SEM) and Energy-Dispersive X-ray spectroscopy (EDS) data for 70% AN sintered at 1700°C [111]; (e) Toughening mechanisms in TiB_2-based composites reinforced by hybrid SiCw and MLG [112]; (f) The fracture surfaces micrographs (FESEM) of TSS samples [113].

However, it has been reported that the additions of Ni, Co or even Fe will lead to the formation of undesirable secondary borides (mainly of the type M_2B, M_3B_2 and $M_{23}B_6$) through a chemical reaction with TiB_2, which have a deleterious effect on many properties of the final materials [4]. Therefore, two or more kinds of these metals are used as sintering additives to sinter TiB_2. The TiB_2-based cermets produced by Sánchez et al. contain austenitic or ferritic binder phases within the Fe + Ni system, and the formation of undesirable secondary borides has been totally prevented [114]. In another work, novel TiB_2-based cermets have been consolidated through the hot isostatic pressing of powder mixtures comprising TiB_2 and metallic alloys incorporating Fe, Ni, and Co additives [115]. Removing the τ phase from the binder phase within the TiB_2 cermets leads to a notable enhancement in the composite's toughness without compromising its hardness. Titanium diboride ceramics containing 0.5 wt.% Cr and 0.5 wt.% Fe with a density of 98.8% of the theoretical density was obtained by pressureless sintering at 1900°C. Surprisingly, the mechanical properties of the specimen sintered at 1800°C—exhibiting a strength of 506 MPa and a fracture toughness of 6.16 $MPa{\cdot}m^{1/2}$—proved superior to those observed in the specimen sintered at 1900°C. The increase in temperature caused the abnormal growth of grains, leading to the deterioration of mechanical properties. It is revealed that a Ti–Fe–Cr phase that existed at the triple junction has good wettability with TiB_2. Ti-rich liquid phase enhanced mass transfer to accelerate densification [81]. The simultaneous addition of Ni and Mo improved the density of TiB_2 up to 99.2% [116]. The added Mo can interact with TiB_2 to form a new phase encapsulated on the surface of TiB_2, thus effectively inhibiting the grain growth. In the case of the addition of Ni and Ta, TiB_2 composites showed a significant enhancement (up to 98.1% T.D.) in comparison to the pure TiB_2 (85.6% T.D.) [117].

Recently, high-entropy alloy (HEA) has been gradually applied to ceramics' sintering as a new additive [118, 119]. High-entropy alloy is a novel alloy system that contains five or more metallic elements with equal or nearly equal quantities, which could lower the sintering temperature and inhibit grain growth. It also possesses excellent wettability with ceramic matrix. The substantial mixing entropy from multi-principle elements can cause lattice distortion and hinder cooperative diffusion processes [120, 121]. Hence, High entropy alloy is a promising candidate material for the sintering additives of TiB_2 ceramics. There are some reports about the fabrication of TiB_2 composites using high entropy alloys as sintering additives [122]. Zhao [123] et al. prepared the TiB_2 ceramics with a relative density of 99.1%, a Vickers hardness parameter of 2174.64 HV, and a flexural strength of 427.69 MPa by spark plasma sintering with 10 wt.% HEA ($CoCrFeNiMn_{0.5}Ti_{0.5}$) as sintering additives. The HEA is located at the grain boundaries according to the result of EDS, and it fills the gap among grains and further promotes the densification of ceramic materials.

For metal additives it has experienced a development process from a single component to the multi-components, and high-entropy alloys. However, the addition of metal sintering additives will reduce the high-temperature mechanical properties of TiB_2 for the low melting point of metals, so it cannot be used in the high-temperature fields. Hence, the preference for non-metallic additives arises to enhance sinterability without instigating unwanted grain growth.

5.1.2 Non-Metallic Sintering Additives

Various non-metallic additives (AlN, SiC, Si_3N_4, B_4C, TaC, ZrO_2 et al.) have been used for improving the densification of TiB_2 with good mechanical properties [124, 125]. Non-metal sintering additives

can react with TiO_2/B_2O_3 on the surface of TiB_2 particles to form a second phase with a lower melting point and densify it under the action of LPS.

Murthy and co-workers reported that the sintering, microstructure, and properties of TiB_2 materials were densified using a $MoSi_2$ sinter additive for the first time [126]. It was found that the addition of 10-20 wt.% $MoSi_2$ can achieve 97%-99% ρ_{th} in the composites at 1700°C by hot-pressing. The densification mechanism was dominated by liquid phase sintering in the presence of $TiSi_2$. The formation of $TiSi_2$ has been described by two thermodynamically feasible reactions, as shown in the following two equations.

$$TiO_2 + MoSi_2 \rightarrow TiSi_2 + MoO_3(g) \quad (2)$$

$$TiB_2 + 3O_2(g) + MoSi_2 \rightarrow TiSi_2 + B_2O_3(g) + MoO_3(g) \quad (3)$$

The optimized composite (TiB_2–10 wt.% $MoSi_2$) exhibits a significantly higher hardness (H_v ~26.5 GPa) and modest fracture toughness (K_{IC} ~4.3 MPa $m^{1/2}$). The crack deflection is believed to be the only toughening mechanism. The microstructure of TiB_2 ceramics, when hot pressed using $TiSi_2$ as an additive, demonstrates significant improvements in mechanical properties and oxidation resistance. Specifically, the addition of $TiSi_2$ enhances the mechanical strength of TiB_2 ceramics and imparts superior oxidation resistance compared to TiB_2 + $MoSi_2$ composites, with performance closely matching that of pure TiB_2. This indicates the effectiveness of $TiSi_2$ in promoting densification and improving the overall quality of TiB_2 ceramics [127].

Similarly, for the TiB_2-AlN composite system, it has been reported that the presence of AlN strongly influences on the sinterability and mechanical properties of TiB_2 [128]. The addition of a small amount (≤5 wt.%) of AlN to TiB_2 facilitated the elimination of titania (TiO_2) present on the surface of the TiB_2 powder. This elimination occurred through a reaction between AlN and TiO_2, forming TiN and Al_2O_3. Two thermodynamically feasible reactions have described the formation of TiN:

$$3TiO_2(s) + 4AlN(s) \rightarrow 3TiN(s) + 2Al_2O_3(s) + 1/2N_2(g) \quad (4)$$

$$TiB_2(s) + 3/2N_2(g) \rightarrow TiN(s) + 2BN(s) \quad (5)$$

The elimination of TiO_2 markedly improved the sinterability and mechanical properties of TiB_2. It can be seen that the addition of 5% AlN changed the fracture mode of TiB_2 from the original transgranular fracture to the combined action of transgranular fracture and intergranular fracture. Al_2O_3 and BN were formed during the densification process. However, with an increased addition of AlN (10 wt.%), both sinterability and mechanical properties appeared to decrease, likely attributed to the remaining unreacted AlN. In another work, Antônio et al., shown in Figure 6d, investigated the effect of sintering temperature (1500-1800°C) on the densification behavior of TiB_2-30% AlN by SPS [111].

Upon adding a minor quantity (2.5 wt.%) of Si_3N_4 to TiB_2, the Si_3N_4 underwent a reaction with the surface-bound TiO_2 in the TiB_2 powder, resulting in the formation of titanium nitride, boron nitride, and amorphous silica [129]. In the case of TiB_2-B_4C-Fe sintered compacts, microstructural coarsening resulting from the addition of a larger quantity (5 wt.% Fe) was inhibited by the incorporation of B_4C

particles, and mechanical properties were consequently improved [130]. The effects of EuB_6, NdB_6, and CrB_2 etc., on TiB2 ceramics' densification have been studied [131-133].

According to Namini et al., the effect of SiC addition on microstructural features, phase evolution, and mechanical properties of the vacuum hot-pressed TiB_2 at 1850°C for 2 h under the pressure of 20 MPa was investigated [82]. Indeed, according to reports, SiC reacted with oxide impurities, specifically TiO_2 and B_2O_3, existing on the particle surfaces. The incorporation of SiC particles facilitated the activation of toughening mechanisms, including crack deflection, crack branching, and grain breaking. Ternary TiB_2–WC–TiC ceramic composites were manufactured through hot-pressed sintering. Sintering additives like WC, TiC, Mo, Ni, and Co were incorporated to generate a liquid phase, enhancing densification processes [134]. The microstructure of these composites exhibited a characteristic core/rim configuration, with the core primarily composed of TiB_2 and the rim predominantly consisting of TiC. The fracture mechanism can also be studied [112], and crack bridging occurred, as illustrated in Figure 6e. Possessing a high aspect ratio, hybrid MLG/SiCw had an enlarged contact area with the TiB_2 matrix compared to the conventional toughening phase, increasing the effect of bridging the two sides of the crack. In addition, the impact of Si_3N_4 and SiC additives on the microstructure and sintering behavior of TiB_2-based composites was studied [113]. Accordingly, the flaky-like compounds apparent in the relevant graph (Figure 6f) are associated with the in situ BN and graphite. The sample was fractured transgranularly and intergranularly.

From the above, it must be clear now that the addition of sintering additives has an essential influence on the sinterability and microstructure of the TiB_2. Out of various sintering additives explored for TiB_2, incorporating $TiSi_2$ during consolidation through SPS has been extensively studied and reported to yield the most substantial enhancement in densification and mechanical properties to date. In the past few years, researchers have extensively studied the densification of TiB_2 with silicides and borides as sintering additives. In recent years, more researchers have gradually paid attention to the carbide and nitride systems. The influences of some nitrides and carbides on TiB_2 have been studied extensively. However, in developing these materials, aside from the crucial aspect of sintering temperature, fine-tuning the quantity of the binder is equally critical to achieving higher densification, improved mechanical properties, and finer grain size.

5.2 Anisotropic Particles

The main disadvantage of TiB_2 ceramics in structural applications is its poor fracture toughness. The second phase of sintering additives has been introduced above to increase density and improve performance. Generally speaking, the toughening of particles mainly depends on the residual stress caused by the mismatch of the thermal expansion coefficient [135]. When the size/content of the second-phase particles exceeds a specific limit, the toughening effect will be pretty limited. To further strengthening and toughen, it is necessary to improve the contribution of other toughening mechanisms, such as crack bridging and grain drawing, correspondingly highlighting the necessity of one-dimensional whiskers or fiber-reinforced ceramic materials. For example, using SPS sintering technology, Lin [136] et al. synthesized TiB2-based composites containing 15 wt.% carbon nanotubes. The results showed that introducing carbon nanotubes could improve the mechanical properties of the materials, especially the fracture toughness. Although incorporating carbon nanotubes can achieve good sintering density, the agglomeration of carbon nanotubes and the stability at higher sintering temperatures still need to be solved.

It was found that the addition of SiC particles increases the relative density, and TiB_2 reacts with SiC to form the TiC, which leads to the dissipation of fracture energy in the crack propagation process [137-139]. SiC whiskers and nanowires have better mechanical properties, heat resistance, corrosion resistance, and high-temperature oxidation resistance [140]. These excellent properties make SiC whiskers and nanowires important in the strengthening and toughening of ceramic materials and composites. Yan [141] et al. conducted a comparative study introducing varying volume percentages of SiCw and SiCp to TiB_2, evaluating their sinterability and subsequent mechanical properties. The findings indicated that the addition of SiCp facilitated an intergranular fracture mode, whereas the inclusion of SiCw encouraged a transgranular mode. By contrast, the most significant Vickers hardness and fracture toughness values were obtained for the specimen containing 25 wt.% SiCw for 29.3 GPa, and 6.1 $MPa{\cdot}m^{1/2}$, respectively. Deng et a. found that the fracture toughness of the TiB_2 with the addition of 30 wt.% SiCw increased from 3.4 $MPa{\cdot}m^{1/2}$ to 7.8 $MPa{\cdot}m^{1/2}$ compared with the monolithic TiB_2 by the hot-pressed sintering [142]. The observed toughening mechanisms likely stemmed from crack deflection around the whiskers and the phenomenon of whisker bridging, primarily facilitated by whisker pullout. Farhadi et al. discovered that the enhancement in fracture toughness resulted from the toughening and strengthening effects induced by SiC whiskers, particularly through mechanisms like crack deflection. Moreover, their findings indicated that the enhanced densification of TiB_2-SiC ceramic composites was attributed to the addition of SiC whiskers. These whiskers facilitated the reduction of oxide impurities by reacting with them and subsequently removing them from the surface layer of TiB_2 particles. According to the above discussion, SiCw exhibits excellent enhancement of the comprehensive mechanical properties of TiB_2.

Compared with SiC whiskers, SiC nanowires have higher aspect ratio and better mechanical properties. Therefore, SiC nanowires as reinforcing and toughening reinforcers have a better prospect in the application of composites [143]. It has been reported that the addition of SiCnw can enhance the mechanical properties of Si_3N_4 and Al_2O_3 [144, 145], but there are almost no relevant reports on SiCnw-enhanced TiB_2.

5.3 Texture Processing

The control of microstructure has become the primary method to improve the properties of materials. Since the microstructure largely determines TiB_2 ceramics' properties, various techniques can be used to tailor the microstructure of TiB_2. For example, a textured microstructure is developed to have excellent anisotropic properties, broadening their application fields [146]. The methods to prepare the textured ceramics mainly include hot-forging [146, 147], templated grain growth [148, 149], and magnetic alignment [150]. The first two methods can only produce textured ceramics with simple shapes due to their own preparation methods. However, these limitations can be overcome by the magnetic alignment technology. Many methods are carried out to prepare highly textured TiB_2, such as the preferred orientation of grain in the direction of applied pressure during hot pressing [151] (Figure 7a). The rod-like or plate-like grains can be in-situ synthesized and formed under pressure orientation during spark plasma sintering [152] or by slip-casting in a strong magnetic field [153].

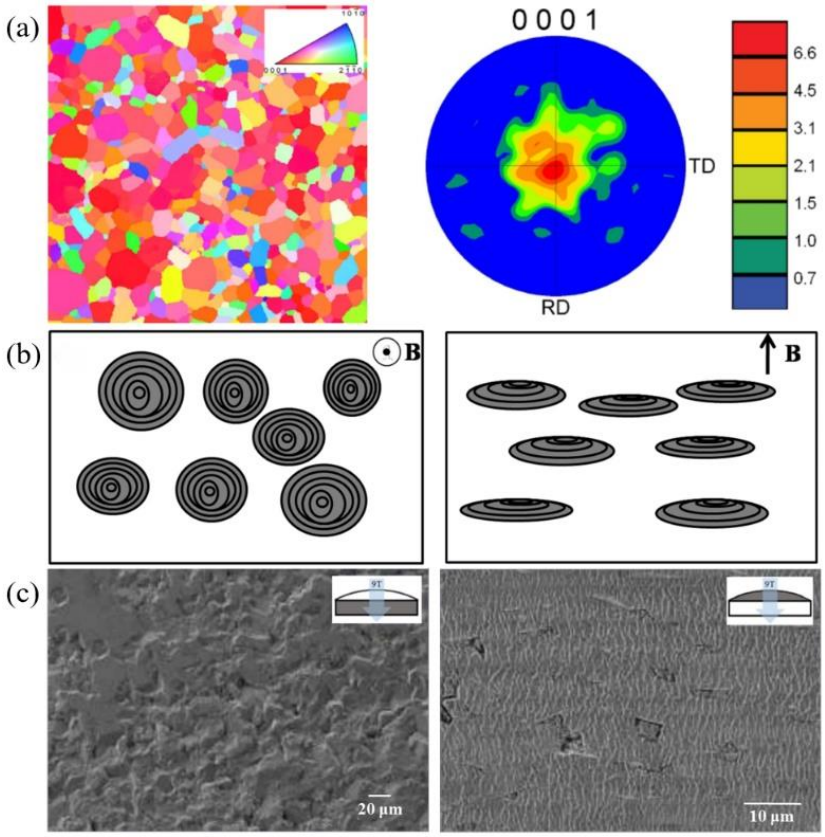

Figure 7 Texture processing image of TiB_2: (a) Crystal orientation map and pole figure of the surface normal to the hotpressing direction in the TiB_2 material hot pressed at 1800°C [151]. (b) Schematic images of TiB_2 grain orientation in 6 T [153]. (c) The SEM images of the worn tracks after the tribological tests of the textured TiB_2 material [154].

The Lotgering factor usually determines the quantitative evaluation of orientation/texture degree. The higher the Lotgering factor, the higher the orientation/texture degree. The Lotgering factor of the sample with random orientation is 0, while that of the sample with fully textured/oriented (transverse isotropic) is 1 [146, 155]. Ran et al. successfully prepared the textured TiB_2 monolithic ceramics in a one-step in situ synthesis and densification process. The Lotgering orientation factors of the sample were 0.68. However, no samples with significant anisotropy and high texture characteristics were formed [152].

The addition of an external magnetic field can solve this problem well. Indeed, Strong Magnetic Field Alignment (SMFA) is a relatively recent technique harnessing the anisotropy of magnetic susceptibility in non-cubic lattices. When antimagnetic or paramagnetic particles within a liquid medium are exposed to a magnetic field, they have the capability to reorient themselves by an angle to reduce the overall energy of the system [146, 147]. Sakka et al. had shown that dense ceramics with high texture (polymerization coefficient in the range of 0.89-0.94) could be prepared by colloidal process under magnetic solid field conditions [147].

Yang et al. successfully prepared highly c-axis textured TiB_2 ceramics by slip-casting in a strong magnetic field of 6 T and subsequent pressureless sintering [153], with Y_2O_3 and Al_2O_3 as the sintering additives. When samples were prepared by magnetic texturing treatment, the orientation factor is 0.80. After sintering without a magnetic field, the texture degree is 0.94 due to the effect of grain growth. It is also found that the microstructure of TiB_2 ceramics on different surfaces has

noticeable texture differences due to the other grain orientations. Based on this, the schematic images of TiB_2 grain orientation in 6 T were shown in Figure 7b. However, the relative density of the sample is low (~55%).

Recently, Tatarko and co-workers have successfully prepared highly textured TiB_2 ceramics by slip casting an aqueous suspension in a magnetic field of 9T, followed by using Field Assisted Sintering Technology (FAST). The sintered material displayed a Lotgering orientation factor of 0.90, indicating a notable alignment. In this case, the c-axis of TiB_2 was oriented parallel to both the magnetic field and the FAST pressing direction. In addition, the mechanical properties of highly textured and dense TiB_2 (RD ≥ 98%) were also reported. The mechanical properties of textured TiB_2 materials showed apparent anisotropy. The hardness and elastic modulus measured along C axis of TiB_2 were 37% and 13% higher than those along C axis, respectively [154] (Figure 6c).

The magnetic alignment will be widely used in preparing textured TiB_2 ceramics due to its advantages of grain shape independence and application to refined nanocrystalline grains in the future. More researchers should pay more attention to studying TiB_2 with high texture microstructure, high density, and excellent mechanical properties.

6. High-Temperature Mechanical Properties

To realize the application of TiB_2 in ultra-high temperature fields, it is far from enough only at room temperature to obtain better comprehensive performance, these properties must be maintained at higher temperatures. Therefore, it is essential to maintain good chemical stability, hardness, strength, and oxidation resistance at high temperatures. This section mainly discusses the research status of these properties.

Thermal hardness testing has been widely used to evaluate various ceramics' high temperature mechanical behavior. The thermal hardness test can reflect the change of material strength with temperature well and predict the creep property of materials. Nakano et al. measured microhardness on TiB_2 single crystals between room temperature and 1000°C [156]. They reported that the dislocation glide on the {1010} [0001] slip system was the primary slip system above 500°C. For monolithic TiB_2, it retained a maximum hardness of ~5 GPa at 800°C [9].

It is commonly noted that the relationship between temperature and hardness is exponential, which is expressed by the following formula:

$$H_v = H_0 \exp[-(T - T_0)/\tau] \quad (6)$$

H_V is Vickers hardness. H_0 generally refers to the hardness at 0 K (intrinsic hardness). T_0 and T generally refer to room temperature and test temperature, respectively. τ is the empirical coefficient. For TiB_2, its hardness decreases more obviously with the increase of temperature.

The type and composition of the second phase additive greatly influence the hardness of TiB_2 at room temperature and high temperature. It was observed that the hot hardness of TiB_2 varied between 7.3 GPa [TiB_2-5 wt.% (Fe-Fe_2B)] and 4.8 GPa [TiB_2-20 wt.% (Fe-CrNi-Fe_2B)] at 800°C [9]. Adding silicon-based sintering additive to TiB_2 will make the hardness of TiB_2 remain high value at high-temperature. TiB_2-2.5 wt.% $MoSi_2$ reportedly had the maximum hardness of 27.6 GPa at room temperature (RT) and retained a hardness of 10.5 GPa up to 900°C [157].

The high-temperature strength of TiB_2 increases gradually with the gradual increase of temperature. This transformation law was also reported by Munro et al. [9] as well as Baumgartner

et al. [80]. The strength increase was attributed to the alleviation of residual internal stresses. These stresses originated from the anisotropic thermal expansion of the microcrystalline constituent particles and were further mitigated by crack healing induced by oxidation processes.

The high-temperature hardness, composition, phase composition, and microscopic size of the sintering additives and the second phase all have a great influence on the high-temperature strength of TiB_2. Therefore, choosing suitable sintering additives is necessary to improve the high-temperature strength. In another way, Under the action of small amounts of sintering additives, the strength of TiB_2 increases with the increase of temperature (up to 1000°C). However, the addition of large quantities of sintering additives in the TiB_2 will hurt the performance. For example, when larger sintering additive quantity (10 wt.% $MoSi_2$) was introduced into TiB_2, the strength decreased considerably at 1000°C [1]. In recent work, Demirskyi et al. [158] revealed that the strength of prepared TiB_2 by SPS technology could be improved by adding NbB_2 (up to 50 wt.%) even up to 1800°C in Ar environment. These studies demonstrate the potential of TiB_2 composites at elevated temperatures under protective environments.

TiB_2 has good performance at high-temperature, but it is effortless to be oxidized at high temperatures. Therefore, it is necessary to understand the oxidation behavior of TiB_2 ceramics in depth. High-temperature oxidation is a form of corrosion that does not require the presence of a liquid electrolyte. The oxidation mechanism of TiB_2 depends on temperature, partial pressure of oxygen, exposure time, porosity, and the properties of sintering additives [159]. Tampieri et al. researched the oxidation mechanism of monolithic TiB_2 [160]. The temperature at which TiB_2 ceramic starts to oxidize is about 400°C. Oxidation kinetic can be controlled by diffusion up to T ≈ 900°C and in the first stage of the oxidation at 1000 and 1100°C. It is well known that TiB_2 oxidizes according to the chemical reaction (7).

$$\mathrm{TiB_2} + 5/2\mathrm{O_2} \rightarrow \mathrm{B_2O_3} + \mathrm{TiO_2} \quad (7)$$

The B_2O_3 on the surface of TiB_2 is generally considered as a protective layer below 1000°C. However, when the temperature is too high, B_2O_3 will vaporize and evaporate, leaving only TiO_2 and a large number of pores. In this way, TiB_2 does not have dense oxide layer at high-

temperature, active oxidation will exist with fast and linear kinetics [160]. Therefore, improving the relatively poor high-temperature oxidation resistance is necessary by changing the composition of the originally-formed oxide layer. It has been reported that the oxidation resistance of various TiB_2-based materials reveals that monolithic TiB_2 without sintering additives has poor oxidation resistance compared to TiB_2 with Si- or Al-based sinter-additives [52]. Raju and co-workers prepared TiB_2–$MoSi_2$ composites and studied their oxidation kinetics and mechanisms. The oxidation kinetics was slower for the TiB_2-10 wt.% $MoSi_2$ due to the presence of SiO_2 in the oxide scale. The efficacy of $MoSi_2$ in imparting enhanced oxidation resistance of TiB_2 [161]. Murthy et al. found a new composite of TiB_2 with $CrSi_2$ with excellent oxidation resistance [162]. TiO_2, Cr_2O_3 and SiO_2 were formed in these composite materials with the addition of $CrSi_2$ in the isothermal oxidation process, which has good oxidation resistance. This composite was found to be a superior oxidation-resistant material as compared to other TiB_2 composites with $MoSi_2$, $TiSi_2$, and CrB_2.

7. Conclusions and Outlook

The study reviews various synthesis methods and sintering techniques for TiB_2 and discusses the effects of sintering additives and reinforcements on densification, microstructure, and multiple properties, including high-temperature properties. TiB_2 has excellent mechanical and physical properties such as refractoriness, high hardness, good fracture strength, and significant oxidation resistance. However, enhanced techniques are required to improve the properties due to its poor sintering properties. Most of the basic properties can be further improved by adopting the preferred processing routes, compositions and microstructures required for the development.

In terms of powder synthesis routes, the main synthesis methods are solid-phase synthesis, liquid-phase synthesis and gas-phase synthesis. Solid-phase synthesis methods include the traditional reduction method, self-propagating high-temperature synthesis (SHS), high-energy ball milling, and metal-thermal reduction etc. The advantage is that the reaction conditions are relatively mild, and the disadvantage is that the reaction rate is slower, the powder particles are coarse, and the purity is lower. Liquid-phase synthesis methods include sol-gel method, molten salt method, etc., the advantages of which are faster reaction rate, fine powder particles, and higher purity, the disadvantage of which is that the reaction conditions are relatively harsh, requiring the use of special solvents or catalysts. Unlike the traditional high-temperature reduction process, the molten salt-assisted carbothermal or metal thermal reduction technique has been widely used to synthesize nanoscale non-oxide powders at low temperatures. It has great advantages in synthesizing ultrafine TiB_2 powders.

In terms of sintering techniques, the traditional TiB_2 sintering densification studies, such as pressureless sintering (PS) and hot press sintering (HP) are decreasing. In recent years, novel sintering techniques such as spark plasma sintering (SPS), flash spark plasma sintering (FSPS), near-net-shape colloidal processing, and laser sintering have been applied in non-oxide ceramics. In the future, it will be a trend to investigate the optimization of multi-stage SPS sintering parameters or the combination of multiple advanced sintering techniques to limit some undesirable sintering reactions that may affect the properties of TiB_2-based ceramics.

There are two main categories of additives and enhancers for TiB_2: metallic additives and non-metallic additives. Metal additives include aluminium, nickel, iron, molybdenum, tungsten, etc. Although the study of metal additives in TiB_2 has gone through the process of adding from a single unit to multi-element, high-entropy alloys, which serves to reduce the sintering temperature of TiB_2, promote the densification of TiB_2, and improve the electrical conductivity and toughness of TiB_2, the high-temperature performance and oxidative stability of TiB_2 will also be reduced. Non-metallic additives, including carbon, nitrogen, silicon, oxygen, etc., role is to improve the high-temperature performance and oxidative stability of TiB_2, but at the same time, will also affect the densification and conductivity of TiB_2, in terms of non-metallic sintering additives, despite the great efforts made in the development of the material. Still, so far the success achieved in the improvement of the scope of the improvement is limited to the improvement of the toughness of the TiB_2 material and the improvement of sintering properties is not enough. The type, form, and content of ceramic sintering additives are critical to the development of dense TiB_2 ceramics with good properties.

It is well known that TiB_2 ceramics, as a high-temperature structural material, has a broad potential for application. The future development trend of TiB_2 is mainly manifested in the following aspects: firstly, the new synthesis method will make use of chemical reaction, biological templates,

microwave radiation and other techniques to control the particle size, morphology, distribution and composition of TiB_2 in order to prepare TiB_2 nanomaterials with special structure and function; secondly, the new sintering technology will make use of advanced equipment to improve the toughness and sinterability of TiB_2 materials. sintering technologies will use advanced equipment, sintering modes and parameters to optimize the sintering process of TiB_2 and improve its density, homogeneity and consistency; thirdly, novel additives and reinforcing agents will balance the various properties of TiB_2 through the synergistic effect of metallic or non-metallic materials to achieve its multifunctionality; lastly, the novel application areas of TiB_2 will take advantage of its excellent properties to develop new TiB_2-based composites, coating materials, catalytic materials, sensing materials, etc., to expand its applications in energy, environment, medical, information and other fields. However, it also has some problems and challenges, such as sintering difficulties, low flexural strength and fracture toughness, which limit its application in some fields. Moreover, measurements of mechanical properties at high temperatures are scarce. In addition, most of the studies on TiB_2 oxidation have been performed by isothermal or continuous heating. No more advanced tests can better replicate the actual conditions (e.g. extreme or harsh environments at ultra-high temperatures) in the relevant applications. Therefore, from an application point of view, such tests are very important and must be performed. These test methods need to be adapted to assess the stability of the underlying microstructure under such extreme conditions.

Author Contributions

Xinran Lv: Conceptualization, Investigation, Methodology, Writing - original draft. Ziqiang Yin: Data curation, Writing - review & editing. Zhigang Yang: Data curation, Validation, Writing - review & editing. Junshuai Chen: Data curation, Investigation, Writing - review & editing. Shen Zhang: Investigation, Writing - review & editing. Shaolei Song: Conceptualization, Data curation, Writing - review & editing. Gang Yu: Methodology, Writing - review & editing.

Competing Interests

The authors have declared that no competing interests exist.

References

1. Golla BR, Mukhopadhyay A, Basu B, Thimmappa SK. Review on ultra-high temperature boride ceramics. Prog Mater Sci. 2020; 111: 100651.
2. Levine SR, Opila EJ, Halbig MC, Kiser JD, Singh M, Salem JA. Evaluation of ultra-high temperature ceramics foraeropropulsion use. J Eur Ceram Soc. 2002; 22: 2757-2767.
3. Monteverde F. Progress in the fabrication of ultra-high-temperature ceramics: “In Situ” synthesis, microstructure and properties of a reactive hot-pressed HfB_2–SiC composite. Compos Sci Technol. 2005; 65: 1869-1879.
4. Basu B, Raju GB, Suri AK. Processing and properties of monolithic TiB_2 based materials. Int Mater Rev. 2013; 51: 352-374.
5. Cutler RA. Engineering properties of borides. In: ASTM Engineered Materials Handbook, Vol. 4 Ceramics and Glasses. Almere, Netherlands: ASM International; 1991. pp. 787-803.

6. Upadhya KY, Yang JM, Hoffman W. Materials for ultrahigh temperature structural applications. Am Ceram Soc Bull. 1997; 76: 51-56.
7. Chamberlain AL, Fahrenholtz WG, Hilmas GE, Ellerby DT. High-strength zirconium diboride-based ceramics. J Am Ceram Soc. 2004; 87: 1170-1172.
8. Ramberg JR, Williams WS. High temperature deformation of titanium diboride. J Mater Sci. 1987; 22: 1815-1826.
9. Munro RG. Material properties of titanium diboride. J Res Natl Inst Stand Technol. 2000; 105: 709.
10. Ramberg JR, Wolfe CF, Williams WS. Resistance of titanium diboride to high-temperature plastic yielding. J Mater Sci. 1985; 68: C-78-C-79.
11. Zhang G, Yue X, Jin Z, Dai J. In-situ synthesized TiB_2 toughened SiC. J Eur Ceram Soc. 1996; 16: 409-412.
12. He Q, Wang A, Liu C, Wang W, Wang H, Fu Z. Microstructures and mechanical properties of B_4C-TiB_2-SiC composites fabricated by ball milling and hot pressing. J Eur Ceram Soc. 2018; 38: 2832-2840.
13. Verma V, Cheverikin V, Câmara Cozza R. Review: Effect on physical, mechanical, and wear performance of ZrB_2-based composites processed with or without additives. Int J Appl Ceram Technol. 2020; 17: 2509-2532.
14. Bansal NP. Handbook of ceramic composites. Boston, MA: Kluwer Academic Publishers; 2005.
15. Tallon C, Franks GV. Chapter 5-Near-net-shaping of ultra-high temperature ceramics. In: Ultra-high temperature ceramics: Materials for extreme environment applications. Wiley; 2014. pp. 83-111.
16. Cotton J. Ultra-high-temperature ceramics. Adv Mater Process. 2010; 168: 26-28. Available from: https://www.researchgate.net/publication/283809047_Ultra-High-Temperature_Ceramics.
17. Justin J, Jankowiak A. Ultra high temperature ceramics: Densification, properties and thermal stability. Aerospace Lab. 2011; 3: 1-11. Available from: https://www.researchgate.net/publication/280953124_Ultra_High_Temperature_Ceramics_Densification_Properties_and_Thermal_Stability.
18. Wuchina E, Opila E, Opeka M, Fahrenholtz B, Talmy I. UHTCs: Ultra-high temperature ceramic materials for extreme environment applications. Electrochem Soc Interface. 2007; 16: 30.
19. Telle R. Boride and carbide ceramics. In: Materials Science and Technology. Wiley; 2006.
20. Murray J, Liao P, Spear K. The B-Ti (boron-titanium) system. Bull Alloy Phase Diagr. 1986; 7: 550-555.
21. Milman V, Warren M. Elastic properties of TiB_2 and MgB_2. J Phys Condens Matter. 2001; 13: 5585.
22. Liang H, Chen H, Peng F, Liu L, Li X, Liu K, et al. High-pressure strength and compressibility of titanium diboride (TiB_2) studied under non-hydrostatic compression. J Phys Chem Solids. 2018; 121: 256-260.
23. Akopov G, Yeung MT, Kaner RB. Rediscovering the crystal chemistry of borides. Adv Mater. 2017; 29: 1604506.
24. Okamoto NL, Kusakari M, Tanaka K, Inui H, Otani S. Anisotropic elastic constants and thermal expansivities in monocrystal CrB_2, TiB_2, and ZrB_2. Acta Mater. 2010; 58: 76-84.

25. Peng F, Fu HZ, Cheng XL. First-principles calculations of thermodynamic properties of TiB_2 at high pressure. Phys B Condens Matter. 2007; 400: 83-87.
26. Will G. Electron deformation density in titanium diboride chemical bonding in TiB_2. J Solid State Chem. 2004; 177: 628-631.
27. Raju G, Basu B. Development of high temperature TiB_2-based ceramics. Key Eng Mater. 2009; 395: 89-124.
28. Lee K, Kang SH, Kim DJ. Enhanced sintering of TiB_2 with SiC addition prepared by polycarbosilane infiltration. Key Eng Mater. 2005; 287: 102-107.
29. Takahashi T, Itoh H. Ultrasonic chemical vapor deposition of TiB_2 thick films. J Cryst Growth. 1980; 49: 445-450.
30. Bates SE, Buhro WE, Frey CA, Sastry SM, Kelton K. Synthesis of titanium boride $(TiB)_2$ nanocrystallites by solution-phase processing. J Mater Res. 1995; 10: 2599-2612.
31. Kravchenko S, Torbov V, Shilkin S. Preparation of titanium diboride nanopowder. Inorg Mater. 2010; 46: 614-616.
32. Chen L, Gu Y, Qian Y, Shi L, Yang Z, Ma J. A facile one-step route to nanocrystalline TiB_2 powders. Mater Res Bull. 2004; 39: 609-613.
33. Axelbaum RL, DuFaux DP, Frey CA, Kelton KF, Lawton SA, Rosen LJ, et al. Gas-phase combustion synthesis of titanium boride (TiB_2) nanocrystallites. J Mater Res. 1996; 11: 948-954.
34. Gu Y, Qian Y, Chen L, Zhou F. A mild solvothermal route to nanocrystalline titanium diboride. J Alloys Compd. 2003; 352: 325-327.
35. Lu S, Sun S, Huang X, Tu G, Zhu X, Li K. Deposition behavior of TiB_2 by microwave heating chemical vapor deposition (CVD). Green Process Synth. 2015; 4: 203-208.
36. Nozari A, Ataie A, Heshmati-Manesh S. Synthesis and characterization of nano-structured TiB_2 processed by milling assisted SHS route. Mater Charact. 2012; 73: 96-103.
37. Liu L, Aydinyan S, Minasyan T, Hussainova I. SHS produced TiB_2-Si powders for selective laser melting of ceramic-based composite. Appl Sci. 2020; 10: 3283.
38. Oghenevweta J, Wexler D, Calka A. Sequence of phase evolution during mechanically induced self-propagating reaction synthesis of TiB and TiB_2 via magnetically controlled ball milling of titanium and boron powders. J Alloys Compd. 2017; 701: 380-391.
39. Qin Z, Zhang J, Wang J, Ke C. Novel sustainable silicothermic synthesis of phase-pure TiB_2 fine powder. J Alloys Compd. 2020; 834: 155213.
40. Liu J, Liu J, Zeng Y, Zhang H, Li Z. Low-temperature high-efficiency preparation of TiB_2 micro-platelets via boro/carbothermal reduction in microwave heated molten salt. Materials. 2019; 12: 2555.
41. Song S, Zhang T, Xie C, Zhou J, Li R, Zhen Q. Growth behavior of TiB_2 hexagonal plates prepared via a molten-salt-mediated carbothermal reduction. J Am Ceram Soc. 2020; 103: 719-723.
42. Zhang Y, Yang Y, Sun H, Wang J. Synthesis of TiB_2 powders with hexagonal morphology by Sol–Gel method. J Nanosci Nanotechnol. 2019; 19: 7886-7891.
43. Radev D, Marinov M. Properties of titanium and zirconium diborides obtained by self-propagated high-temperature synthesis. J Alloys Compd. 1996; 244: 48-51.
44. Welham NJ. Formation of nanometric TiB_2 from TiO_2. J Am Ceram Soc. 2000; 83: 1290-1292.
45. Kang SH, Kim BS, Kim DJ. The atmosphere effect on synthesis of TiB_2 particles by carbothermal reduction. Mater Sci Forum. 2007; 534: 145-148.

46. Guo WM, Zhang GJ, You Y, Wu SH, Lin HT. TiB_2 powders synthesis by borothermal reduction in TiO_2 under vacuum. J Am Ceram Soc. 2014; 97: 1359-1362.
47. Zeng LY, Wei WX, Sun SK, Guo WM, Li H, Lin HT. Powder characteristics, sinterability, and mechanical properties of TiB_2 prepared by three reduction methods. J Am Ceram Soc. 2019; 102: 4511-4519.
48. Nishiyama K, Nakamur T, Utsumi S, Sakai H, Abe M. Preparation of ultrafine boride powders by metallothermic reduction method. J Phys Conf Ser. 2009; 176: 012043.
49. İpekçi M, Acar S, Elmadağlı M, Hennicke J, Balcı Ö, Somer M. Production of TiB_2 by SHS and HCl leaching at different temperatures: Characterization and investigation of sintering behavior by SPS. Ceram Int. 2017; 43: 2039-2045.
50. Khanra A, Godkhindi M, Pathak L. Sintering behaviour of ultra-fine titanium diboride powder prepared by self-propagating high-temperature synthesis (SHS) technique. Mater Sci Eng A. 2007; 454: 281-287.
51. Tang WM, Zheng ZX, Wu YC, Wang JM, Jun LÜ, Liu JW. Synthesis of TiB_2 nanocrystalline powder by mechanical alloying. T Nonferr Metal Soc. 2006; 16: 613-617.
52. Ricceri R, Matteazzi P. A fast and low-cost room temperature process for TiB_2 formation by mechanosynthesis. Mater Sci Eng A. 2004; 379: 341-346.
53. Kim JW, Shim JH, Ahn JP, Cho YW, Kim JH, Oh KH. Mechanochemical synthesis and characterization of TiB_2 and VB_2 nanopowders. Mater Lett. 2008; 62: 2461-2464.
54. Rabiezadeh A, Hadian A, Ataie A. Preparation of alumina/titanium diboride nano-composite powder by milling assisted sol–gel method. Int J Refract Hard Met. 2012; 31: 121-124.
55. Yu J, Ma L, Zhang Y, Gong H, Zhou L. Synthesis of TiB_2 powders via carbothermal reduction of TiO_2, HBO_2 and carbon black. Ceram Int. 2016; 42: 5512-5516.
56. Yu J, Ma L, Abbas A, Zhang Y, Gong H, Wang X, et al. Carbothermal reduction synthesis of TiB_2 ultrafine powders. Ceram Int. 2016; 42: 3916-3920.
57. Bao K, Wen Y, Khangkhamano M, Zhang S. Low-temperature preparation of titanium diboride fine powder via magnesiothermic reduction in molten salt. J Am Ceram Soc. 2017; 100: 2266-2272.
58. Sahoo S, Singh S. Synthesis of TiB_2 by extended arc thermal plasma. Ceram Int. 2017; 43: 15561-15566.
59. Shahbahrami B, Fard FG, Sedghi A. The effect of processing parameters in the carbothermal synthesis of titanium diboride powder. Adv Powder Technol. 2012; 23: 234-238.
60. Liu D, Chu Y, Jing S, Ye B, Zhou X. Low-temperature synthesis of ultrafine TiB_2 nanopowders by molten-salt assisted borothermal reduction. J Am Ceram Soc. 2018; 101: 5299-5303.
61. Krutskii YL, Bannov AG, Antonova EV, Sokolov VV, Pichugin AY, Maksimovskii EA, et al. Synthesis of fine dispersed titanium diboride from nanofibrous carbon. Ceram Int. 2017; 43: 3212-3217.
62. Subramanian C, Murthy TC, Suri A. Synthesis and consolidation of titanium diboride. Int J Refract Hard Met. 2007; 25: 345-350.
63. Ma L, Yu J, Guo X, Xie B, Gong H, Zhang Y, et al. Preparation and sintering of ultrafine TiB_2 powders. Ceram Int. 2018; 44: 4491-4495.
64. Rodeghiero E, Moore B, Wolkenberg B, Wuthenow M, Tse O, Giannelis E. Sol–gel synthesis of ceramic matrix composites. Mater Sci Eng A. 1998; 244: 11-21.
65. Zhang H, Li F. Preparation and microstructure evolution of diboride ultrafine powder by sol–gel and microwave carbothermal reduction method. J Sol Gel Sci Technol. 2008; 45: 205-211.

66. Carlsson M, Johnsson M. Synthesis and characterisation of TiB_2 whiskers. In: 24th Annual Conference on Composites, Advanced Ceramics, Materials, and Structures: B: Ceramic Engineering and Science Proceedings. Hoboken, NJ, USA: John Wiley & Sons, Inc.; 2000. pp. 375-382.
67. Krishnarao R, Subrahmanyam J. Studies on the formation of TiB_2 through carbothermal reduction of TiO_2 and B_2O_3. Mater Sci Eng A. 2003; 362: 145-151.
68. Hu J, Peng H, Wang S, Guo W, Hu C, Tian X. Synthesis of TiC–TiB_2 composite powders via carbothermal reduction and its reaction mechanism. Adv Appl Ceram. 2017; 116: 409-417.
69. Bača Ľ, Stelzer N. Adapting of sol–gel process for preparation of TiB_2 powder from low-cost precursors. J Eur Ceram Soc. 2008; 28: 907-911.
70. Baik S, Becher PF. Effect of oxygen contamination on densification of TiB_2. J Am Ceram Soc. 1987; 70: 527-530.
71. Wang W, Fu Z, Wang H, Yuan R. Influence of hot pressing sintering temperature and time on microstructure and mechanical properties of TiB_2 ceramics. J Eur Ceram Soc. 2002; 22: 1045-1049.
72. Telle R. Analysis of pressureless sintering of titanium diboride ceramics with nickel, cobalt, and tungsten carbide additives. J Eur Ceram Soc. 2019; 39: 2266-2276.
73. Fu Z, Koc R. Pressureless sintering of TiB_2 with low concentration of Co binder to achieve enhanced mechanical properties. Mater Sci Eng A. 2018; 721: 22-27.
74. Foong LK, Xu C. Hot pressing and microstructural characterization of SiC and TiN added TiB_2 ceramics. Ceram Int. 2021; 47: 3946-3954.
75. Singarapu B, Galusek D, Durán A, Pascual MJ. Glass-ceramics processed by spark plasma sintering (SPS) for optical applications. Appl Sci. 2020; 10: 2791.
76. Nguyen VH, Asl MS, Mahaseni ZH, Germi MD, Delbari SA, Van Le Q, et al. Role of co-addition of BN and SiC on microstructure of TiB_2-based composites densified by SPS method. Ceram Int. 2020; 46: 25341-25350.
77. Zapata-Solvas E, Bonilla S, Wilshaw PR, Todd RI. Preliminary investigation of flash sintering of SiC. J Eur Ceram Soc. 2013; 33: 2811-2816.
78. Failla S, Fu S, Sciti D, Grasso S. Flash spark plasma sintering of pure TiB_2. Open Ceram. 2021; 5: 100075.
79. Demirskyi D, Agrawal D, Ragulya A. Tough ceramics by microwave sintering of nanocrystalline titanium diboride ceramics. Ceram Int. 2014; 40: 1303-1310.
80. Baumgartner H, Steiger R. Sintering and properties of titanium diboride made from powder synthesized in a plasma-arc heater. J Am Ceram Soc. 1984; 67: 207-212.
81. Kang SH, Kim DJ, Kang ES, Baek SS. Pressureless sintering and properties of titanium diboride ceramics containing chromium and iron. J Am Ceram Soc. 2001; 84: 893-895.
82. Namini AS, Gogani SN, Asl MS, Farhadi K, Kakroudi MG, Mohammadzadeh A. Microstructural development and mechanical properties of hot pressed SiC reinforced TiB_2 based composite. Int J Refract Hard Met. 2015; 51: 169-179.
83. Rangaraj L, Divakar C, Jayaram V. Processing of refractory metal borides, carbides and nitrides. Key Eng Mater. 2009; 395: 69-88.
84. Fahrenholtz WG, Hilmas GE, Talmy IG, Zaykoski JA. Refractory diborides of zirconium and hafnium. J Am Ceram Soc. 2007; 90: 1347-1364.

85. Zhang G, Jin Z, Yue X. Reaction synthesis of TiB_2-SiC composites from TiH_2-Si-B_4C. Mater Lett. 1995; 25: 97-100.
86. Nguyen TP, Pazhouhanfar Y, Delbari SA, Van Le Q, Shaddel S, Namini AS, et al. Role of nano-diamond addition on the characteristics of spark plasma sintered TiC ceramics. Diam Relat Mater. 2020; 106: 107828.
87. Fattahi M, Mohammadzadeh A, Pazhouhanfar Y, Shaddel S, Asl MS, Namini AS. Influence of SPS temperature on the properties of TiC-SiCw composites. Ceram Int. 2020; 46: 11735-11742.
88. Munir ZA, Anselmi-Tamburini U, Ohyanagi M. The effect of electric field and pressure on the synthesis and consolidation of materials: A review of the spark plasma sintering method. J Mater Sci. 2006; 41: 763-777.
89. Zhang Z, Shen X, Wang F, Lee S, Wang L. Densification behavior and mechanical properties of the spark plasma sintered monolithic TiB_2 ceramics. Mater Sci Eng A. 2010; 527: 5947-5951.
90. Reddy KM, Kumar N, Basu B. Inhibition of grain growth during the final stage of multi-stage spark plasma sintering of oxide ceramics. Scr Mater. 2010; 63: 585-588.
91. Reddy KM, Kumar N, Basu B. Innovative multi-stage spark plasma sintering to obtain strong and tough ultrafine-grained ceramics. Scr Mater. 2010; 62: 435-438.
92. Maity TN, Gopinath NK, Biswas K, Basu B. Spark plasma sintering of ultrahigh temperature ceramics. In: Spark plasma sintering of materials: Advances in processing and applications. Springer; 2019. pp. 369-440.
93. Jain D, Reddy KM, Mukhopadhyay A, Basu B. Achieving uniform microstructure and superior mechanical properties in ultrafine grained TiB_2–$TiSi_2$ composites using innovative multi stage spark plasma sintering. Mater Sci Eng A. 2010; 528: 200-207.
94. Karthiselva N, Murty B, Bakshi SR. Low temperature synthesis of dense TiB_2 compacts by reaction spark plasma sintering. Int J Refract Hard Met. 2015; 48: 201-210.
95. Balcı Ö, Burkhardt U, Schmidt M, Hennicke J, Yağcı MB, Somer M. Densification, microstructure and properties of TiB_2 ceramics fabricated by spark plasma sintering. Mater Charact. 2018; 145: 435-443.
96. Rosenberger A, Brennan R, Vennila-Raju S, Fry AL. Flash Sintering of Boron Carbide (B_4C). Fort Belvoir, VA: Defense Technical Information Center; 2020.
97. Grasso S, Saunders T, Porwal H, Cedillos-Barraza O, Jayaseelan DD, Lee WE, et al. Flash spark plasma sintering (FSPS) of pure ZrB_2. J Am Ceram Soc. 2014; 97: 2405-2408.
98. Wu J, Niu B, Zhang F, Lei L, Zhang J, Ren L, et al. Effect of titanium diboride on the homogeneity of boron carbide ceramic by flash spark plasma sintering. Ceram Int. 2018; 44: 15323-15330.
99. McKinnon R, Grasso S, Tudball A, Reece MJ. Flash spark plasma sintering of cold-Pressed TiB_2-hBN. J Eur Ceram Soc. 2017; 37: 2787-2794.
100. Agrawal D. Microwave sintering of ceramics, composites, metals, and transparent materials. J Mater Educ. 1997; 19: 49-58.
101. Agrawal DK. Microwave processing of ceramics: A review. Curr Opin Solid State Mater Sci. 1998; 3: 480-485.
102. Demirskyi D, Cheng J, Agrawal D, Ragulya A. Densification and grain growth during microwave sintering of titanium diboride. Scr Mater. 2013; 69: 610-613.
103. Sánchez J, Azcona I, Castro F. Mechanical properties of titanium diboride based cermets. J Mater Sci. 2000; 35: 9-14.

104. Zhang J, Fu Z, Wang W, Wang H. Wettability between TiB_2 ceramic and metals. Acta Metall Sin. 1999; 12: 395.
105. Ghetta V, Gayraud N, Eustathopoulos N. Wetting of iron on sintered TiB_2. Solid State Phenom. 1992; 25: 105-114.
106. Kang ES, Jang CW, Lee CH, Kim CH, Kim DK. Effect of iron and boron carbide on the densification and mechanical properties of titanium diboride ceramics. J Am Ceram Soc. 1989; 72: 1868-1872.
107. Ferber MK, Becher PF, Finch CB. Effect of microstructure on the properties of TiB_2 ceramics. J Am Ceram Soc. 1983; 66: C-2-C-3.
108. Einarsrud MA, Hagen E, Pettersen G, Grande T. Pressureless sintering of titanium diboride with nickel, nickel boride, and iron additives. J Am Ceram Soc. 1997; 80: 3013-3020.
109. Yang HY, Wang Z, Yue X, Ji PJ, Shu SL. Simultaneously improved strength and toughness of in situ bi-phased TiB_2–Ti (C,N)–Ni cermets by Mo addition. J Alloys Compd. 2020; 820: 153068.
110. Jaroszewicz J, Michalski A. Preparation of a TiB_2 composite with a nickel matrix by pulse plasma sintering with combustion synthesis. J Eur Ceram Soc. 2006; 26: 2427-2430.
111. Júnior LAF, Tomaz ÍV, Oliveira MP, Simão L, Monteiro SN. Development and evaluation of TiB_2–AlN ceramic composites sintered by spark plasma. Ceram Int. 2016; 42: 18718-18723.
112. Sun J, Zhao J, Huang Z, Yan K, Jian Y, Yang H. Hybrid multilayer graphene and SiC whisker reinforced TiB_2 based nano-composites by two-step sintering. J Alloys Compd. 2021; 856: 157283.
113. Nguyen VH, Delbari SA, Ahmadi Z, Namini AS, Van Le Q, Shokouhimehr M, et al. Effects of discrete and simultaneous addition of SiC and Si_3N_4 on microstructural development of TiB_2 ceramics. Ceram Int. 2021; 47: 3520-3528.
114. Sánchez J, Barandika M, Gil-Sevillano J, Castro F. Consolidation, microstructure and mechanical properties of newly developed TiB_2-Based materials. Scr Metall Mater. 1992; 26: 957-962.
115. González R, Barandika MG, Ona D, Sánchez JM, Villellas A, Valea A, et al. New binder phases for the consolidation of TiB_2 hardmetals. Mater Sci Eng A. 1996; 216: 185-192.
116. Zhang J, Zhengyi F, Weiming W, Hao W. Microstructure and mechanical properties of TiB_2/(Ni + Mo) composites fabricated by hot pressing. J Mater Sci Technol. 2000; 16: 634.
117. Bača Ľ, Lenčéš Z, Jogl C, Neubauer E, Vitkovič M, Merstallinger A, et al. Microstructure evolution and tribological properties of TiB_2/Ni–Ta cermets. J Eur Ceram Soc. 2012; 32: 1941-1948.
118. Zhu G, Liu Y, Ye J. Fabrication and properties of Ti(C,N)-based cermets with multi-component AlCoCrFeNi high-entropy alloys binder. Mater Lett. 2013; 113: 80-82.
119. Chen CS, Yang CC, Chai HY, Yeh JW, Chau JL. Novel cermet material of WC/multi-element alloy. Int J Refract Hard Met. 2014; 43: 200-204.
120. Yeh JW, Chen SK, Lin SJ, Gan JY, Chin TS, Shun TT, et al. Nanostructured high-entropy alloys with multiple principal elements: Novel alloy design concepts and outcomes. Adv Eng Mater. 2004; 6: 299-303.
121. Koch CC. Nanocrystalline high-entropy alloys. J Mater Res. 2017; 32: 3435-3444.
122. Ji W, Zhang J, Wang W, Wang H, Zhang F, Wang Y, et al. Fabrication and properties of TiB_2-based cermets by spark plasma sintering with CoCrFeNiTiAl high-entropy alloy as sintering aid. J Eur Ceram Soc. 2015; 35: 879-886.
123. Zhao K, Niu B, Zhang F, Zhang J. Microstructure and mechanical properties of spark plasma sintered TiB_2 ceramics combined with a high-entropy alloy sintering aid. Adv Appl Ceram. 2017; 116: 19-23.

124. Telle R, Meyer S, Petzow G, Franz E. Sintering behaviour and phase reactions of TiB_2 with ZrO_2 additives. Mater Sci Eng A. 1988; 105: 125-129.
125. Mokhayer MM, Kakroudi MG, Milani SS, Ghiasi H, Vafa NP. Investigation of AlN addition on the microstructure and mechanical properties of TiB_2 ceramics. Ceram Int. 2019; 45: 16577-16583.
126. Murthy TC, Basu B, Balasubramaniam R, Suri A, Subramanian C, Fotedar R. Processing and properties of TiB_2 with $MoSi_2$ sinter-additive: A first report. J Am Ceram Soc. 2006; 89: 131-138.
127. Murthy TC, Subramanian C, Fotedar RK, Gonal MR, Sengupta P, Kumar S, et al. Preparation and property evaluation of TiB_2 + $TiSi_2$ composite. Int J Refract Hard Met. 2009; 27: 629-636.
128. Li LH, Kim HE, Kang ES. Sintering and mechanical properties of titanium diboride with aluminum nitride as a sintering aid. J Eur Ceram Soc. 2002; 22: 973-977.
129. Park JH, Koh YH, Kim HE, Hwang CS, Kang ES. Densification and mechanical properties of titanium diboride with silicon nitride as a sintering aid. J Am Ceram Soc. 1999; 82: 3037-3042.
130. Tuffe S, Dubois J, Fantozzi G, Barbier G. Densification, microstructure and mechanical properties of TiB_2-B_4C based composites. Int J Refract Hard Met. 1996; 14: 305-310.
131. Murthy TC, Sonber JK, Vishwanadh B, Nagaraj A, Sairam K, Bedse RD, et al. Densification, characterization and oxidation studies of novel TiB_2 + EuB_6 compounds. J Alloys Compd. 2016; 670: 85-95.
132. Murthy TC, Sonber J, Subramanian C, Fotedar R, Gonal M, Suri A. Effect of CrB_2 addition on densification, properties and oxidation resistance of TiB_2. Int J Refract Hard Met. 2009; 27: 976-984.
133. Murthy TC, Sonber J, Subramanian C, Hubli R, Krishnamurthy N, Suri A. Densification and oxidation behavior of a novel TiB_2–$MoSi_2$–CrB_2 composite. Int J Refract Hard Met. 2013; 36: 243-253.
134. Song J, Huang C, Lv M, Zou B, Wang S, Wang J, et al. Effects of TiC content and melt phase on microstructure and mechanical properties of ternary TiB_2-based ceramic cutting tool materials. Mater Sci Eng A. 2014; 605: 137-143.
135. Dai J, Pineda EJ, Bednarcyk BA, Singh J, Yamamoto N. Micromechanics-based simulation of B_4C-TiB_2 composite fracture under tensile load. J Eur Ceram Soc. 2022; 42: 6364-6378.
136. Lin J, Yang Y, Zhang H, Wu Z, Huang Y. Effect of sintering temperature on the mechanical properties and microstructure of carbon nanotubes toughened TiB_2 ceramics densified by spark plasma sintering. Mater Lett. 2016; 166: 280-283.
137. Zhao G, Huang C, Liu H, Zou B, Zhu H, Wang J. Microstructure and mechanical properties of hot pressed TiB_2–SiC composite ceramic tool materials at room and elevated temperatures. Mater Sci Eng A. 2014; 606: 108-116.
138. Singlard M, Tessier-Doyen N, Chevallier G, Oriol S, Fiore G, Vieille B, et al. Spark plasma sintering and mechanical properties of compounds in TiB_2-SiC pseudo-diagram. Ceram Int. 2018; 44: 22357-22364.
139. Sulima I, Putyra P, Hyjek P, Tokarski T. Effect of SPS parameters on densification and properties of steel matrix composites. Adv Powder Technol. 2015; 26: 1152-1161.
140. Yang GZ, Cui H, Sun Y, Gong L, Chen J, Jiang D, et al. Simple catalyst-free method to the synthesis of β-SiC nanowires and their field emission properties. J Phys Chem C. 2009; 113: 15969-15973.
141. Yan SR, Lyu Z, Foong LK. Effects of SiC amount and morphology on the properties of TiB_2-based composites sintered by hot-pressing. Ceram Int. 2020; 46: 18813-18825.

142. Deng J, Ai X. Microstructure and mechanical properties of hot-pressed TiB_2–SiCw composites. Mater Res Bull. 1998; 33: 575-582.
143. Liu Y, Dong L, Lu J, Huo W, Du Y, Zhang W, et al. Microstructure and mechanical properties of SiC nanowires reinforced titanium matrix composites. J Alloys Compd. 2020; 819: 152953.
144. Wang B, Shangguan D, Qiao R, Zhang F, Bai Y, Wang Z, et al. Fabrication, mechanical properties and thermal shock resistance of a dense SiC NWs/α-Si_3N_4 composite coating for protecting porous Si_3N_4 ceramics. Ceram Int. 2019; 45: 23241-23247.
145. Zhang M, Li Z, Wang T, Ding S, Qiu G, Zhao J, et al. High yield synthesis of SiC nanowires and their mechanical performances as the reinforcement candidates in Al_2O_3 ceramic composite. J Alloys Compd. 2019; 780: 690-696.
146. Zhang GJ, Ni DW, Zou J, Liu HT, Wu WW, Liu JX, et al. Inherent anisotropy in transition metal diborides and microstructure/property tailoring in ultra-high temperature ceramics—A review. J Eur Ceram Soc. 2018; 38: 371-389.
147. Zhu X, Sakka Y. Textured silicon nitride: Processing and anisotropic properties. Sci Technol Adv Mater. 2008; 9: 033001.
148. Wu C, Li S, Sassa K, Chino Y, Hattori K, Asai S. Theoretical analysis on crystal alignment of feeble magnetic materials under high magnetic field. Mater Trans. 2005; 46: 1311-1317.
149. Uchikoshi T, Suzuki T, Okuyama H, Sakka Y. Fabrication of textured alumina by electrophoretic deposition in a strong magnetic field. J Mater Sci. 2004; 39: 861-865.
150. Suzuki TS, Uchikoshi T, Sakka Y. Fabrication of textured α-SiC using colloidal processing and a strong magnetic field. Mater Trans. 2007; 48: 2883-2887.
151. Jensen MS, Einarsrud MA, Grande T. Preferential grain orientation in hot pressed TiB_2. J Am Ceram Soc. 2007; 90: 1339-1341.
152. Ran S, Zhang L, Van der Biest O, Vleugels J. Pulsed electric current, in situ synthesis and sintering of textured TiB_2 ceramics. J Eur Ceram Soc. 2010; 30: 1043-1047.
153. Yang Z, Yu J, Deng K, Ren Z, Fu H. Preparation of c-axis textured TiB_2 ceramics by a strong magnetic field of 6 T assisted slip-casting process. Mater Lett. 2018; 217: 96-99.
154. Tatarko P, Grasso S, Kovalčíková A, Medveď D, Dlouhý I, Reece M. Highly textured and strongly anisotropic TiB_2 ceramics prepared using magnetic field alignment (9 T). J Eur Ceram Soc. 2020; 40: 1111-1118.
155. Wu WW, Sakka Y, Estili M, Suzuki TS, Nishimura T, Zhang GJ. Microstructure and high-temperature strength of textured and non-textured ZrB_2 ceramics. Sci Technol Adv Mater. 2013; 15: 014202.
156. Kikuo N, Hiromi M. High temperature hardness of titanium diboride single crystal. Jpn J Appl Phys. 1974; 13: 1005-1006.
157. Raju G, Mukhopadhyay A, Biswas K, Basu B. Densification and high-temperature mechanical properties of hot pressed TiB_2-(0-10 wt.%) $MoSi_2$ composites. Scr Mater. 2009; 61: 674-677.
158. Demirskyi D, Solodkyi I, Nishimura T, Vasylkiv OO. Fracture and property relationships in the double diboride ceramic composites by spark plasma sintering of TiB_2 and NbB_2. J Am Ceram Soc. 2019; 102: 4259-4271.
159. Koh YH, Kim HW, Kim HE. Improvement in oxidation resistance of TiB_2 by formation of protective SiO_2 layer on surface. J Mater Res. 2001; 16: 132-137.
160. Tampieri A, Bellosi A. Oxidation of monolithic TiB_2 and of Al_2O_3-TiB_2 composite. J Mater Sci. 1993; 28: 649-653.

161. Raju GB, Basu B, Suri AK. Oxidation kinetics and mechanisms of hot-pressed TiB_2–$MoSi_2$ composites. J Am Ceram Soc. 2008; 91: 3320-3327.
162. Murthy TC, Sonber JK, Subramanian C, Fotedar RK, Kumar S, Gonal MR, et al. A new TiB_2 + $CrSi_2$ composite–Densification, characterization and oxidation studies. Int J Refract Hard Met. 2010; 28: 529-540.